THE JOURNAL OF PHYSICAL CHEMISTRY B



Feature Article

# A Dozen Years of Single-Molecule Spectroscopy in Physics, Chemistry, and Biophysics

W. E. Moerner

*J. Phys. Chem. B*, **2002**, 106 (5), 910-927• DOI: 10.1021/jp012992g • Publication Date (Web): 12 January 2002

FEATURE ARTICLE

# A Dozen Years of Single-Molecule Spectroscopy in Physics, Chemistry, and Biophysics

**W. E. Moerner***

*Department of Chemistry, Stanford University, Mail Code 5080, Stanford, California 94305-5080*

*Received: August 2, 2001*

Optical spectroscopy at the ultimate limit of a single molecule has grown over the past dozen years into a powerful technique for exploring the individual nanoscale behavior of molecules in complex local environments. Observing a single molecule removes the usual ensemble average, allowing exploration of hidden heterogeneity in complex condensed phases as well as direct observation of dynamical state changes arising from photophysics and photochemistry, without synchronization. This paper reviews single-molecule spectroscopy experiments of the Moerner group, both at liquid helium temperatures and at room temperature, in the areas of physical chemistry, quantum optics, and biophysics. Due to the breadth of applications now appearing, single-molecule spectroscopy may be viewed as a useful new tool for the study of dynamics in complex systems.

## A. Introduction

**1. Why Study Single Molecules in Condensed Phases?** Single-molecule spectroscopy (SMS) allows *exactly one* molecule hidden deep within a condensed phase sample to be observed by using tunable optical radiation (Figure 1a). This represents detection and spectroscopy at the ultimate sensitivity level of $\sim 1.66 \times 10^{-24}$ moles of the molecule of interest (1.66 yoctomole), or a quantity of moles equal to the inverse of Avogadro's number. To probe the molecule, a light beam (typically a laser) is used to pump an electronic transition of the one molecule resonant with the optical wavelength (Figure 1b), and the resulting optical absorption is detected either directly[62] or indirectly by fluorescence excitation.[74] Detection of the single molecule of interest must be done in the presence of billions to trillions of solvent or host molecules and in the presence of noise from the measurement itself. The field of SMS has grown over the past decade to the status of a powerful technique for exploring the individual nanoscale behavior of molecules in complex local environments.

How can SMS provide new information? Clearly, standard ensemble measurements that yield the average value of a parameter for a large number of (presumably identical) copies of the molecule of interest still have great value. By contrast, SMS completely removes the ensemble averaging, which allows construction of a frequency histogram of the actual distribution of values (i.e., the probability distribution function) for an experimental parameter. All would agree that the distribution contains more information than the average value alone. For example, the shape of the full distribution (indeed all the moments of the distribution) can be examined to see if it has multiple peaks or whether it has a strongly skewed shape. Such details of the underlying distribution become crucially important when the system under study is heterogeneous. This would be expected to be the case for many complex condensed matter environments such as real crystals, polymers, or glasses.

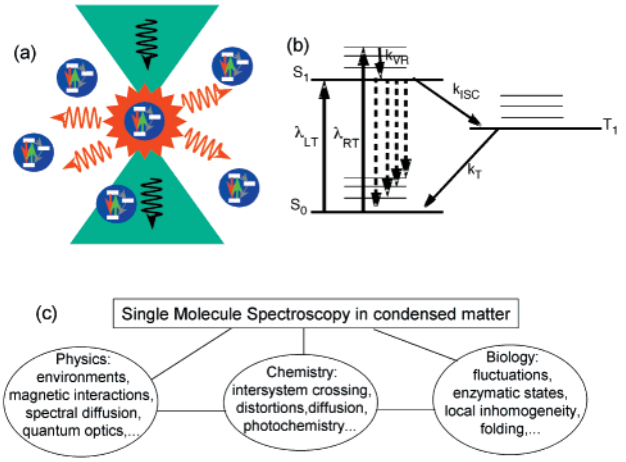


**Figure 1.** (a) Schematic of an optical beam pumping a single resonant molecule, which subsequently either removes photons from the pumping beam or emits fluorescence. (b) Typical energy level scheme for single-molecule spectroscopy. $S_0$, ground singlet state; $S_1$, first excited singlet; $T_1$, lowest triplet state or other intermediate state. For each electronic state, several levels in the vibrational progression are shown. Typical low-temperature studies use wavelength $\lambda_{LT}$ to pump the (0−0) transition, while at room temperature shorter wavelengths $\lambda_{RT}$ are more common. The intersystem crossing or intermediate production rate is $k_{ISC}$, and the triplet decay rate is $k_T$. Fluorescence emission shown as dotted lines originates from $S_1$ and terminates on various vibrationally excited levels of $S_0$ or $S_0$ itself. (c) Some scientific problems in physics, chemistry, and biology that have been explored with single-molecule spectroscopy.

Fortunately, a single molecule can be a local reporter of its "nanoenvironment", that is, of the exact constellation of functional groups, atoms, ions, electrostatic charges, and/or other sources of local fields in its immediate vicinity. For biomolecules, heterogeneity easily arises, for example, if the various individual copies of a protein or oligonucleotide are in different folded states, different configurations, or different stages of an enzymatic cycle.

* Phone: 650-723-1727. Fax: 650-725-0259. E-mail: moerner@stanford.edu.

10.1021/jp012992g CCC: $22.00 
Published on Web 01/12/2002

Another advantage of SMS measurements is that they remove the need for synchronization of many single molecules undergoing a time-dependent process. For example, a large ensemble of molecules undergoing intersystem crossing events must be synchronized in order to measure the triplet lifetime, and this synchronization is only complete at the initial instant. Similarly, an enzymatic system may be in one of several catalytic states, and in an ensemble measurement initial synchronization is required but is quickly lost as the subsequent dynamical transitions of the individual enzymes are stochastic and generally uncorrelated. However, if single copies are observed, any one member of the ensemble is in only one state at a given time, and thus the specific sequence of state changes arising from binding, hydrolysis, and other catalytic steps is available for study. With proper time resolution, rare intermediates can be directly probed, whereas in the ensemble regime these species can be swamped by other, more populated species. Using polarized excitation and polarization analysis of emission, the orientation of a molecular transition dipole can be used to follow mechanical changes such as the motion of biomolecular motors during the force generation process.

A final reason for the use of single-molecule techniques is the possibility of observing new effects in unexplored regimes. For example, several single-molecule systems have unexpectedly shown some form of fluctuating, flickering, or stochastic behavior.[56] The absorption frequency of the single molecule can change as a result of a change in its photophysical parameters or a change in local environment; this behavior has been termed "spectral diffusion" and it can produce spectral shifts or fluctuations. Such fluctuations are now becoming important diagnostics of the single-molecule regime, and they provide unprecedented insight into behavior which is generally obscured by ensemble averaging. On a fundamental level, the time-dependent dynamical behavior of an individual quantum system would be expected to show "quantum jumps"[11,7] as transitions between states occur, and this can be directly observed by SMS techniques.

Stepping back for a moment, it is clear that the past few decades have witnessed a dramatic increase in interest in the "nanoworld" of single atoms, ions, and molecules, for both scientific and technological reasons. Indeed, SMS as defined is related to, but distinct from, several recently successful lines of research on individual species: (i) the spectroscopy of single electrons or ions confined in electromagnetic traps, [34,27,23] (ii) scanning tunneling microscopy (STM)[15] and atomic force microscopy (AFM)[14] of atoms and molecules on surfaces, (iii) the study of ion currents in single transmembrane channels,[85] (iv) single polymer or DNA chains with high concentrations of fluorophores,[77] and (v) force measurements on single molecular motors using optical traps.[18] Perhaps the closest relative to SMS is the area of fluorescence correlation spectroscopy (FCS),[47,105,28] in which dynamical properties are sensed during the diffusion-driven passage of a low concentration of the molecules of interest through the focus of a laser beam. FCS provides useful dynamical information in the ns−ms range, but to obtain a high contrast autocorrelation, the dynamics of many molecules must be summed.

At present, the impact of SMS spans several fields, from physics to chemistry, to biology (Figure 1c), and the number of applications continues to expand. In this paper, selected accomplishments in optical single-molecule detection and spectroscopy are reviewed, with examples taken from the work of the Moerner group at the IBM Almaden Research Center (1987−1995), at the University of California San Diego (1995−1998), and at Stanford University (1998−present). After a brief summary of the introductory concepts, the regime of liquid-helium-temperature spectroscopy of single molecules in solids is described, followed by a summary of more recent room-temperature applications of single-molecule optical techniques to chemical, biophysical, and quantum optical problems. Several comprehensive reviews of this area may be consulted for details beyond the scope of this article and for references to the broad array of work of other investigators. [58,53,55,75,60,10,69,80,109,63,104,3,33,95]

**2. Basic Principles of Single-Molecule Spectroscopy.** To put it simply, to achieve SMS at any temperature, one must (a) guarantee that only one molecule is in resonance in the volume probed by the laser and (b) provide a signal-to-noise ratio (SNR) for the single-molecule signal that is greater than unity for a reasonable averaging time.

Guaranteeing only one molecule in resonance is generally achieved by dilution. For example, at room temperature one need only work with roughly $10^{-10}$ mole/liter concentration in a probed volume of 10 $\mu$m$^3$. At liquid helium temperatures, the phenomenon of inhomogeneous broadening,[92,82,90] (described in the next section) can be used to achieve dilution factors from $\sim 10^4$ to $10^5$ simply by tuning the laser frequency to a spectral region where only one molecule is in resonance.

Achieving the required SNR can be done by several methods. To obtain as large a signal as possible, one needs a combination of small focal volume, large absorption cross section, high photostability, weak bottlenecks into dark states such as triplet states, operation below saturation of the molecular absorption, and high fluorescence quantum yield if fluorescence is detected. For absorption methods, achieving a low noise level from background effects follows from careful reduction of residual signals and operation at a power level sufficient to reduce the relative contribution from laser shot noise. For fluorescence methods, one must rigorously exclude fluorescent impurities, minimize the volume probed to avoid Raman scattering, and scrupulously reject any scattered radiation at the pumping wavelength. (Some details of the considerations that lead to successful SMS will be described in sections B.1−3 below, and the reader is referred to ref 54 for further detail.)

Several optical configurations have been demonstrated to satisfy these basic requirements. At low temperatures, high-resolution optical methods can be applied, such as laser frequency-modulation spectroscopy[62] or fluorescence excitation spectroscopy,[74] and these spectral methods may be combined with microscopy.[4,32] At room temperature, one can detect the burst of light as a molecule passes through the focus of a laser beam,[88] or one can use optical microscopy to observe the same single molecule for an extended period, measuring signal strength, lifetime, polarization, fluctuations, and so on, all as a function of time. Successful microscopic techniques include scanning methods such as near-field scanning optical microscopy (NSOM)[13] and confocal microscopy,[68] as well as the wide-field methods of epifluorescence[99] and total internal reflection microscopy.[26]

### B. Single-Molecule Spectroscopy at Low Temperatures

High-resolution optical spectroscopy of single molecules at low temperatures has led to a variety of new observations, for example, the first direct observation of spectral shifting ("spectral diffusion") of a single molecule due to spontaneous conformational changes of the nearby environment, light-induced spectral shifts, Markovian dynamics, vibrational spectroscopy, and magnetic resonance of a single molecular spin. Measurement of the second-order correlation function of the

**TABLE 1: Low-Temperature Single-Molecule Spectroscopy Milestones**

| experiment | refs |
|---|---|
| Observation of statistical fine structure scaling as $\sqrt{N}$ | 21 |
| Optical detection and spectroscopy of a single molecule in a solid | 62, 35 |
| Optical dephasing, nonlinear optical saturation | 2 |
| Spectral diffusion and measurement of spectral trajectories | 57 ,4, 2 |
| Single molecule in a polymer, photoinduced kinetics | 8, 6 |
| Photon antibunching for a single molecule | 9 |
| Vibrational spectroscopy (resonance Raman) | 96, 98, 67 |
| Magnetic resonance of a single molecular spin | 39 |
| Near-field optical spectroscopy of a single molecule in a solid | 66 |
| Pumping single molecules with morphology-dependent resonances of a microsphere | 72 |

emitted light, $g^{(2)}$, shows the purely quantum-mechanical property of photon antibunching, proving that exactly one molecule is in resonance. Table 1 lists specific SMS milestones of the Moerner group for the low-temperature regime, and a selection of these will now be described.

**1. Early Steps toward Single-Molecule Spectroscopy.** The first steps toward the single-molecule regime arose from work at IBM in the early 1980s on persistent spectral hole-burning effects in the electronic transitions of impurities in solids (for a review, see refs 50 and 90). Briefly, if a molecule with a strong zero-phonon transition and minimal Franck−Condon distortion is doped into a solid and cooled to liquid helium temperatures, the optical absorption becomes inhomogeneously broadened (Figure 2a). The width of the lowest electronic transition for any one molecule becomes very small and can approach the lifetime-limited width of a few MHz because lattice phonons are quenched. At the same time, the different copies of the impurity molecule in the sample acquire slightly different absorption energies due to local strains and other defects in the solid. Spectral hole-burning occurs when light-driven physical or chemical changes are produced only in those molecules resonant with the light, which yields a dip or "spectral hole" in the overall absorption profile that may be used for optical recording of information in the optical frequency domain or for coherent transient effects.

One goal of the research in the Moerner group at IBM was the exploration of ultimate limits to the spectral hole-burning optical storage process. A particularly interesting limit on the signal-to-noise ratio of a spectral hole results from the finite number of molecules that contribute to the absorption line near the hole. Due to unavoidable number fluctuations in the density of molecules in any spectral interval, there should exist a "spectral noise" on an inhomogeneous absorption profile scaling as the square root of the number of molecules in resonance. This effect occurs even if the probability distribution for resonance frequencies is perfectly smooth. We named this effect "statistical fine structure" (SFS), and Figure 2a shows how the relative size of SFS scales as $1/\sqrt{N}$. What is not so well-known about number fluctuations is the fact that the absolute root-mean-square (rms) size of the fine structure scales as $\sqrt{N}$. Surprisingly, prior to the late 1980s, SFS had not been detected.

In 1987, SFS was observed for the first time,[59] using a powerful zero-background absorption technique, laser frequency-modulation (FM) spectroscopy,[16] and a sample composed of pentacene dopant molecules in a transparent *p*-terphenyl crystal. FM spectroscopy probes the sample with a phase-modulated laser beam; when a narrow spectral feature is present, the imbalance in the laser sidebands leads to amplitude modulation in the detected photocurrent at the modulation frequency. A key feature of the method is that it senses only the deviations of the absorption from the average value, so that detection of SFS could be easily accomplished without using ultralow concentrations. In Figure 2b, SFS is the repeatable spectral structure over the entire range of the two laser scans, one of which includes a spectral hole burned at the center, showing directly the that the size of a spectral hole (here the derivative shape) must be larger than the SFS in order to be detected.[51] SFS is clearly an unusual spectral feature, in that its *size* depends not upon the total number of resonant molecules, but rather upon the square root of the number. Due to three factors ($\sqrt{N}$ scaling, insensitivity to any scattering background, and quantum-limited detection sensitivity), FM spectroscopy seemed an appropriate method to push to the single-molecule limit. It must also be stated that the particularly low quantum efficiency for spectral hole-burning ($<10^{-9}$) made pentacene in *p*-terphenyl a critical first choice for a material that would allow single-molecule detection.

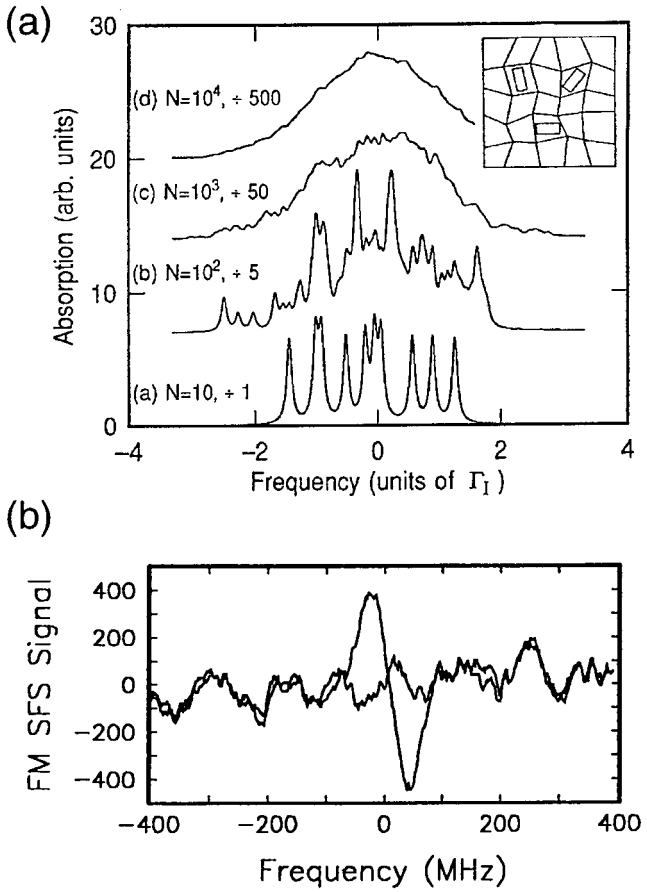


**Figure 2.** (a, upper) Illustration of the underlying source of SFS using simulated absorption spectra with different total numbers of absorbers *N*, where a Gaussian random variable provides center frequencies for the inhomogeneous distribution. Subtraces (a) through (d) correspond to *N* values of 10, 100, 1000, and 10 000, respectively, and the traces have been divided by the factors shown. For clarity, all traces except (a) have been offset vertically, and the homogeneous width was $\gamma_H = \Gamma_I/10$, with $\Gamma_I$ the inhomogeneous width. Inset: several guest impurity molecules are sketched as rectangles with different local environments produced by strains, local electric fields, and other imperfections in the host matrix. (b, lower) SFS detected by FM spectroscopy for pentacene in a *p*-terphenyl crystal at 1.4 K, with a spectral hole at zero relative frequency for one of the two scans. The laser line width is ~3 MHz, and zero frequency is equivalent to 593 nm optical wavelength.

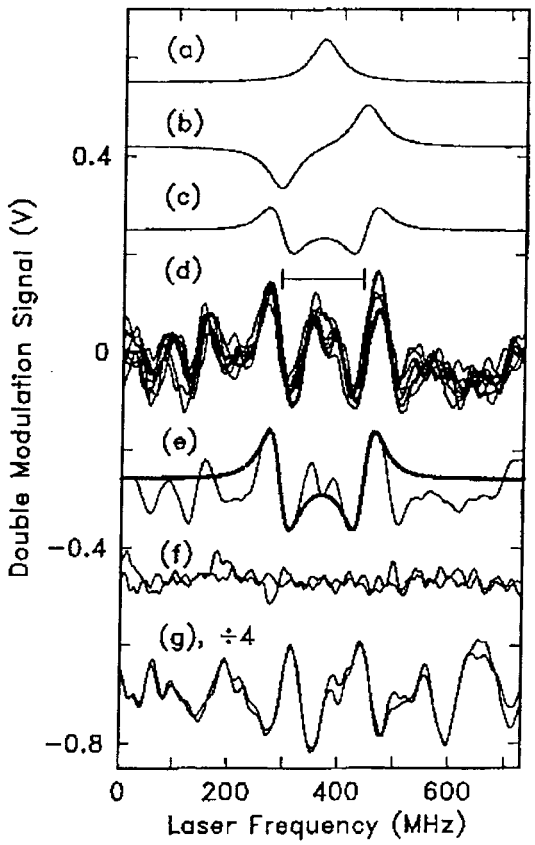


**Figure 3.** Single molecules of pentacene in *p*-terphenyl detected by FM-Stark optical absorption spectroscopy. The "W"-shaped structure in the center of trace (d) is the absorption from a single pentacene molecule. (a) Simulation of absorption line with (power-broadened) line width of 65 MHz. (b) Simulation of FM spectrum for (a), modulation frequency $\omega_m = 75$ MHz. (c) Simulation of FM/Stark line shape. (d) single-molecule spectra at 592.423 nm, 512 averages, 8 traces overlaid, bar shows value of $2\omega_m = 150$ MHz. (e) Average of traces in (d) with fit to the in-focus molecule (smooth curve). (f) Signal far off line at 597.514 nm. (g) Traces of SFS at the $O_2$ line center, 592.186 nm. For details, see ref 62.

**2. Single-Molecule Spectroscopy by Absorption.** The first SMS experiments in 1989 utilized either of two powerful double-modulation absorption techniques, laser frequency-modulation with Stark electric field secondary modulation (FM-Stark) or frequency-modulation with ultrasonic strain secondary modulation (FM-US).[62,61,35,52] Although FM spectroscopy is in principle a zero-background technique, secondary modulation of the absorption feature was required in order to remove the effects of residual amplitude modulation produced by the imperfect phase modulator. In contrast to fluorescence methods, Rayleigh and Raman scattering were unimportant, hence it was not necessary to prepare a sample with high-quality flat surfaces. Figure 3 (specifically the W-shaped structure in trace d) shows examples of the optical absorption spectrum from a single molecule of pentacene in *p*-terphenyl using the FM-Stark method.

Although this early observation and similar data from the FM-US method served to stimulate much further work, there is one important limitation to the general use of FM methods for SMS. As was shown in the early papers on FM spectroscopy,[16,17] extremely low absorption changes as small as $10^{-7}$ can be detected in a 1 s averaging time, but only if large laser powers on the order of several mW can be delivered to the detector to reduce the relative size of the shot noise. This presents a problem for SMS in the following way. For any SMS technique, the laser beam must be focused to a small spot in the sample to maximize the probability of absorption by the molecule given by $\sigma/A$, where $\sigma$ is the absorption cross section and $A$ is the beam area. Small focal spots in the sample mean high intensities, and the power in the laser beam must be maintained below the value that would cause saturation broadening of the single-molecule line shape. As a result, it is quite difficult to utilize laser powers in the mW range for SMS of allowed transitions at low temperatures. In fact, powers below 100 nW are generally required. This is one reason the SNR of the original data on single molecules of pentacene in *p*-terphenyl in Figure 3 was only on the order of 5. (The other reason was the use of relatively thick cleaved samples, which produced a larger number of weak out-of-focus molecules in the probed volume. This problem has been overcome with much thinner samples in modern experiments.) In recent experiments,[36] frequency modulation of the absorption line itself (rather than the laser) was produced by an oscillating (Stark) electric field alone, and this method has also been used to detect the absorption from a single molecule at liquid helium temperatures. While successful, these methods are limited by the quantum shot noise of the laser beam, which is relatively large at the low laser intensity required to prevent saturation of the single-molecule absorption.

**3. Single-Molecule Spectroscopy by Fluorescence Excitation.** The successful observations of SFS and SMS for pentacene in *p*-terphenyl showed that this system has sufficiently weak hole-burning such that it should be a useful model system for single-molecule spectroscopy. In 1990, Orrit et al. demonstrated that fluorescence excitation produces superior signal-to-noise if the emission is collected efficiently and the scattering sources are minimized by the use of ultrathin sublimed crystal platelets.[74] Subsequent experiments have almost exclusively used this method. In fluorescence excitation, a tunable narrow band single-frequency laser is scanned over the absorption profile of the single molecule, and the presence of absorption is detected by measuring the fluorescence emitted. A long-wavelength-pass filter is used to block the pumping laser light, and the fluorescence shifted to long wavelengths from the tunable pump is detected with a photon-counting system. The detection is background-limited and the shot noise of the probing laser is only important for the signal-to-noise of the spectral feature, not the signal to background. For this reason, it is critical to efficiently collect photons (as with a paraboloid or other high numerical aperture collection system) and to reject the pumping laser radiation. To illustrate, suppose a single molecule of pentacene in *p*-terphenyl is probed with 1 mW/cm$^2$ near the onset of saturation of the absorption due to triplet level population. The resulting incident photon flux of $3 \times 10^{15}$ photons/s-cm$^2$ will produce about $3 \times 10^4$ excitations per second. With a fluorescence quantum yield of 0.8 for pentacene, about $2.4 \times 10^4$ emitted photons/s can be expected. At the same time, $3 \times 10^8$ photons/s illuminate the focal spot 3 $\mu$m in diameter. Considering that the resonant 0−0 fluorescence from the molecule must be thrown away along with the pumping light, rejection of the pumping radiation by a factor greater than $10^5$ to $10^6$ is generally required, with minimal attenuation of the fluorescence. This is often accomplished by low-fluorescence glass filters or by holographic notch attenuation filters.

In early experiments on the model system of pentacene in *p*-terphenyl at low pumping intensity, the lifetime-limited homogeneous line width of $7.8 \pm 0.2$ MHz was observed.[57] This line width is the minimum value allowed by the lifetime of the $S_1$ excited state of 24 ns, in agreement with photon echo

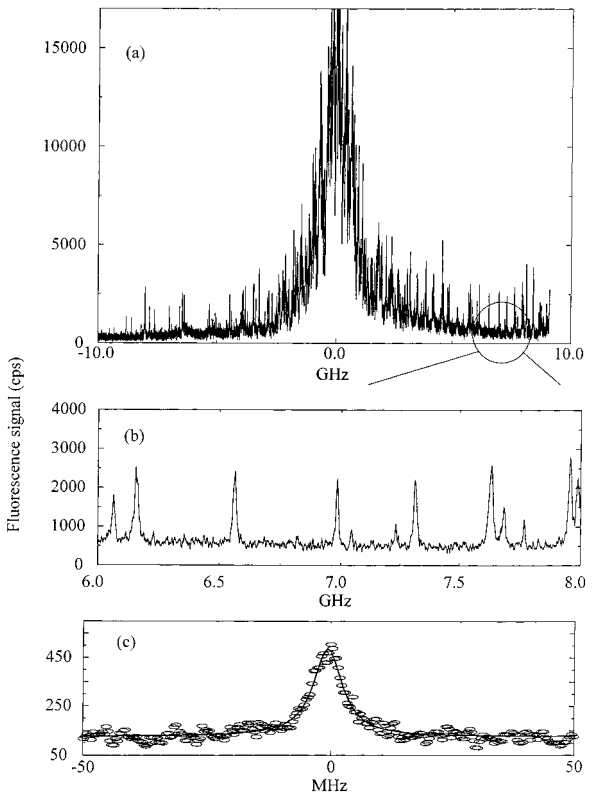


**Figure 4.** Fluorescence excitation spectra for pentacene in *p*-terphenyl at 1.5 K measured with a tunable dye laser of line width ~3 MHz. The laser detuning frequency is referenced to the line center at 592.321 nm. (a) Broad scan of the inhomogeneously broadened line; all the sharp features are repeatable structure. (b) Expansion of 2 GHz spectral range showing several single molecules. (c) Low-power scan of a single molecule at 592.407 nm showing the lifetime-limited width of 7.8 MHz and a Lorentzian fit. After ref 53.

measurements on large ensembles.[76,22] Such narrow single-molecule absorption lines are wonderful for the spectroscopist: many detailed studies of the local environment can be performed, because such narrow lines are much more sensitive to local perturbations than are broad spectral features. A graphic experimental demonstration of the difference between the inhomogeneous line profile and the homogeneous absorption profiles of individual molecules is shown in Figure 4.

A hybrid image of a single molecule can be obtained by acquiring optical spectra as a function of the position of the laser focal spot in the sample. Figure 5 (left side) shows such a three-dimensional "pseudo-image" of single molecules of pentacene in *p*-terphenyl.[4] The *z*-axis of the image is the (Stokes-shifted) fluorescence emission signal, the horizontal axis is the laser frequency detuning (300 MHz range), and the axis going into the page is one transverse spatial dimension produced by scanning the laser focal spot (40 $\mu$m range). For sections of this image along the spatial dimension the single molecule is actually serving as a highly localized nanoprobe of the laser beam diameter itself (here ~5 $\mu$m). However, in the frequency dimension the features are fully resolved as the laser line width is negligible (~3 MHz).

Single-molecule spectra as a function of laser intensity provide details of the (incoherent) saturation behavior and the influence of the dark triplet state dynamics. Figure 5 (right side) shows both the line width and the detected emission rate for three single molecules in the wings of the inhomogeneous line, yielding a (free-space) value for the saturation intensity of $I_s$ = 2.5 mW/cm$^2$. This value is smaller than expected from the ensemble-measured intersystem crossing parameters,[2] indicating that the individual molecules experience modifications due to differences in local environments. In the high-intensity limit, the peak fluorescence emission rate saturates at 7.2 ± 0.7 × $10^5$ photons/s (panel b), and the homogeneous line width broadens according to the expected form (solid curve in panel a) showing dephasing effects produced by coupling to a local phonon mode.[2] These measurements on individual molecules are complementary to earlier studies of line widths of spectral holes in solids, which naturally contain contributions from many molecules.

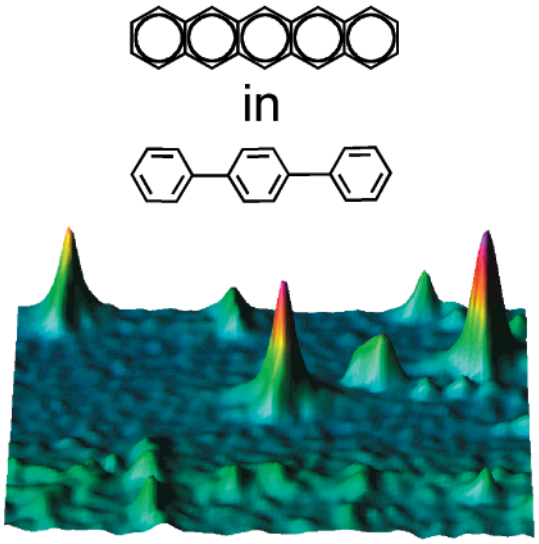


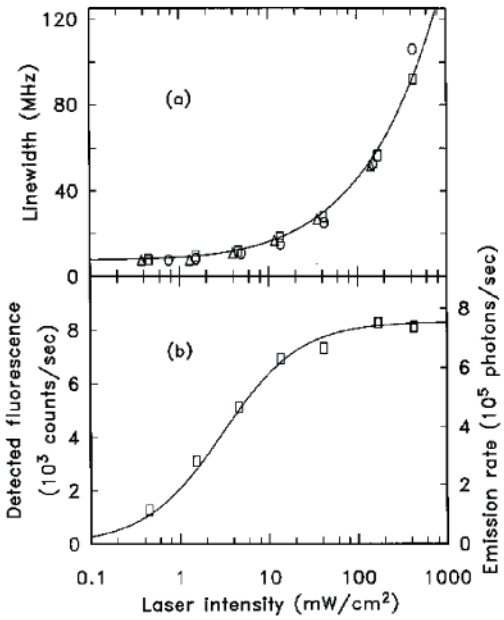


**Figure 5.** (left side) Three-dimensional pseudo image of single molecules of pentacene in *p*-terphenyl. The measured fluorescence signal (z-axis) is shown over a range of 300 MHz in excitation frequency (horizontal axis, center = 592.544 nm) and 40 $\mu$m in spatial position (axis into the page). (right side) Optical saturation behavior of the line width (a) and emission rate (b) for single molecules of pentacene in *p*-terphenyl. For details, see ref 2.

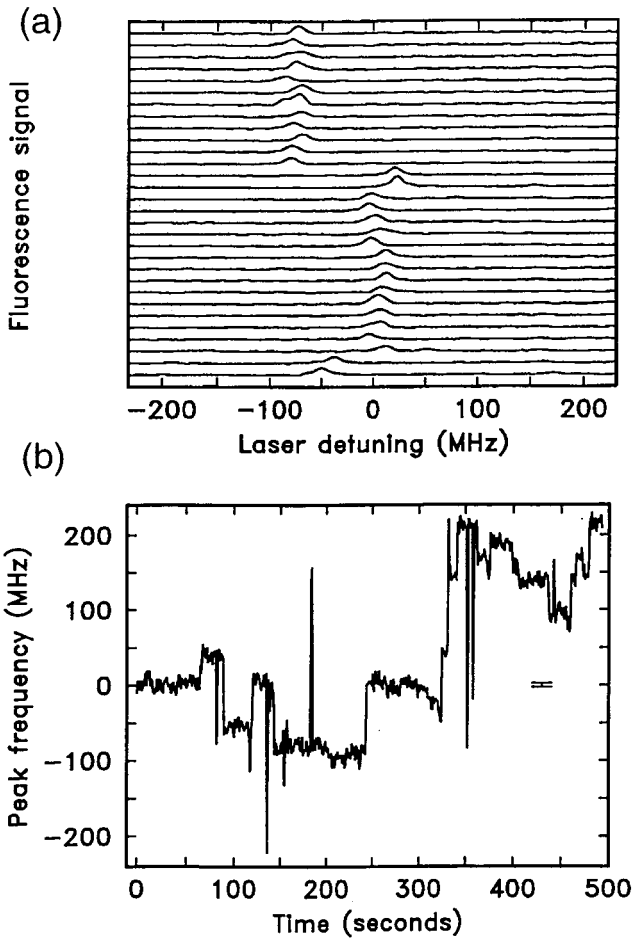


**Figure 6.** Examples of single-molecule spectral diffusion for pentacene in *p*-terphenyl at 1.5 K. (a) A series of fluorescence excitation spectra, each 2.5 s long spaced by 0.25 s showing discontinuous shifts in resonance frequency, with zero detuning = 592.546 nm. (b) Trend or trajectory of the resonance frequency over a long time scale for the molecule in (a). For details, see ref 4.

**4. Observation of Spectral Diffusion of a Single Molecule.** In the course of the early SMS studies on pentacene in *p*-terphenyl in the Moerner group, an unexpected phenomenon appeared: dramatic resonance frequency shifts of individual pentacene molecules in a crystal at 1.5 K.[57,4] Even though this behavior is not diffusion in the strict sense, i.e., it is not governed by a diffusion equation, the effect is termed "spectral diffusion" in deference to related shifting behavior long postulated for impurity molecules in amorphous systems.[30] Here, spectral diffusion means changes in the center (resonance) frequency of the probe molecule due to configurational changes in the nearby host that affect the frequency of the electronic transition via guest−host coupling, strain fields, etc. For example, Figure 6a shows a sequence of fluorescence excitation spectra of a single pentacene molecule in *p*-terphenyl taken as fast as allowed by the tunable laser and the available SNR. The spectral shifting or hopping of this molecule from one resonance frequency to another from scan to scan is clearly evident.

Spectral shifting can be studied by (a) recording the observed line shapes for many single molecules,[8] (b) autocorrelation,[110] and (c) measurement of the *spectral trajectory* $\omega_o(t)$.[4] To record $\omega_o(t)$, one analyzes many sequentially acquired fluorescence excitation spectra, such as those in Figure 6a, and plots a trajectory or trend of the center frequency versus time as shown in Figure 6b. The spectral trajectory shows that, for this molecule, the optical transition energy appears to have a preferred set of values and performs spectral jumps between these values that are discontinuous on the 2.5 s time resolution of the measurement. The behavior of other single molecules was qualitatively and quantitatively different, ranging from wandering to creeping.[2] This is a direct demonstration of hidden heterogeneity from molecule to molecule that can only be observed by SMS; such spectral trajectories cannot be obtained when a large ensemble of molecules is in resonance. The spectral jumps for different molecules are generally uncorrelated, thus the behavior of an ensemble-averaged quantity such as a spectral hole in this system would show only a broadening and smearing of the line.

The first question that should be asked when such behavior is observed is this: is the effect spontaneous, occurring even in the absence of the probing laser radiation, or is it light-driven, i.e., produced by the optical excitation itself? To distinguish spontaneous vs light-driven behavior, the spectral diffusion effect was explored as a function of laser power, and, for pentacene in *p*-terphenyl crystals, the effect was found to be predominantly spontaneous. Since the single-molecule absorption is extremely sensitive to the local strain field, it is reasonable to expect that the spectral jumps are due to internal dynamics of some configurational degrees of freedom in the surrounding lattice, driven by the phonons present at the experimental temperature. The situation is analogous to that for amorphous systems, where the local dynamics that perturbs probe molecules results from the two-level systems near the guest. The dynamics results from phonon-assisted tunneling or thermally activated barrier crossing. One possible source for the tunneling states in the crystalline system could be discrete torsional librations of the central phenyl ring of the nearby *p*-terphenyl molecules about the molecular axis. The *p*-terphenyl molecules in a domain wall between two twins or near lattice defects may have lowered barriers to such central-ring tunneling motions. Using this model, an insightful theoretical study by J. L. Skinner et al. of the spectral diffusion trajectories[83,84,31,89] has allowed determination of specific constellations of defects that can produce the observed behavior. The detailed theoretical analysis depended upon the availability of the full spectral trajectory, thus attesting to the power of SMS in probing details of the local nanoenvironment.

Spectral shifts of single-molecule line shapes are common in many systems, appearing not only for certain crystalline hosts, but also for essentially all polymers studied (*vide infra*), and even for polycrystalline Shpol'skii matrices.[81] Moreover, spectral shifting has been observed on a much larger frequency scale for single molecules on surfaces at room temperature for both near-field[100] and far-field methods.[108] This behavior is turning out to be a ubiquitous feature of single-molecule experiments,[56] giving us a new window into local dynamical behavior.

**5. Single Molecules in Polymers: Light-Induced Spectral Shifts.** The experiments described so far were performed with single impurity molecules doped into a crystalline matrix. Amorphous systems such as glasses or polymers have a number of interesting physical properties at low temperatures that are quite different from those for crystalline materials, in particular a complex, multidimensional potential energy surface.[79] According to the two-level system (TLS) model, the material can be approximated by a distribution of asymmetric double-well potentials in which only the two lowest energy levels of each double-well are important. The effect of these TLSs on thermal and optical properties has been an area of extensive study.[90] In 1992, perylene doped into a poly(ethylene) matrix became the first polymeric system to allow SMS.[8,6] Spectral diffusion

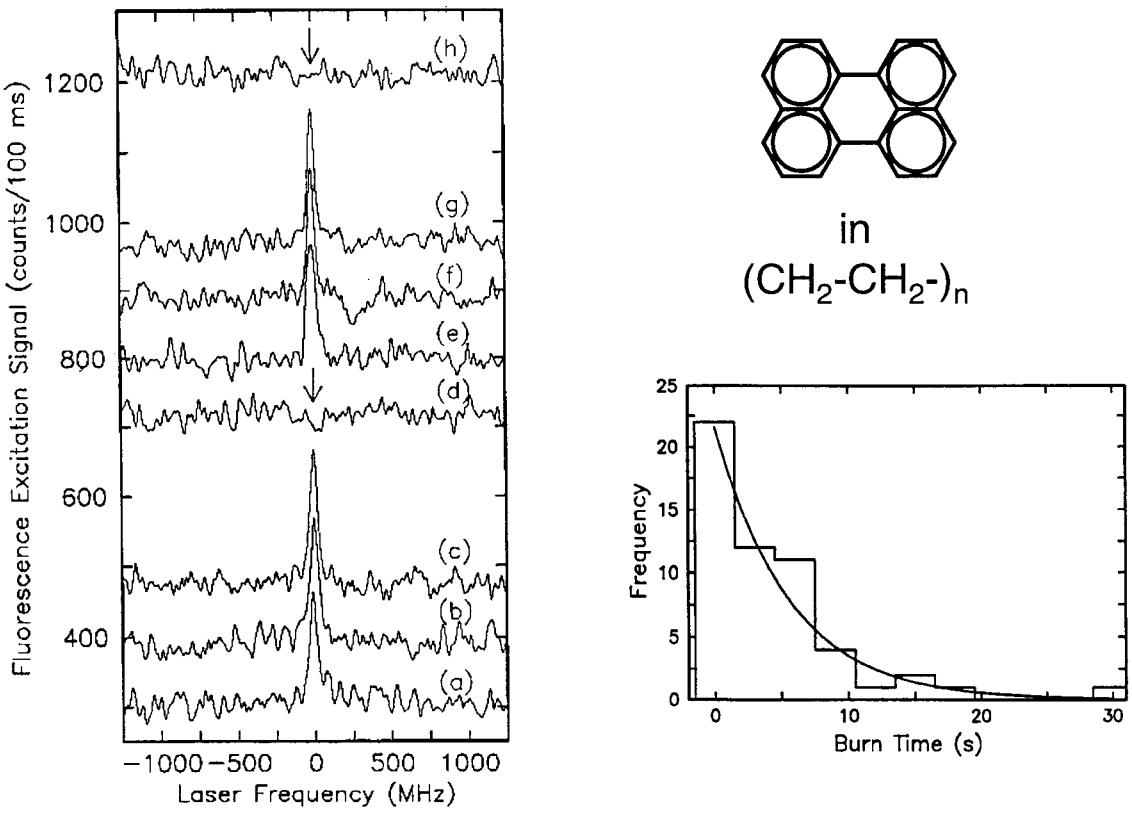


**Figure 7.** Left side: Illustration of light-induced reversible frequency shifting for a single molecule of perylene in poly(ethylene) at 1.4 K. Right side: Histogram of waiting times before the spectral shift (hole-burning), from 53 events for the same single perylene molecule. For details, see refs 6 and 8.

manifested itself in this system in two different ways: as discontinuous jumps in frequency space on the scale of several hundred MHz, similar to pentacene in *p*-terphenyl discussed above, and in addition, the observed line widths varied from molecule to molecule due to fast shifts of small amplitude.

Light-driven shifts in absorption frequency were also observed, in which the rate of the process clearly increased with increases in laser intensity. This effect may be called "spectral hole-burning" by analogy with the earlier hole-burning literature;[50] however, since here only one molecule is in resonance with the laser, the absorption line simply disappears. An example is presented in Figure 7, left side. Traces a, b, and c show three scans of one perylene molecule. After trace c the laser was tuned into resonance with the molecule until the fluorescence dropped to the background level (hole-burning). Trace d was then acquired, which showed that the resonance frequency shifted by more than ±1.25 GHz as a result of the light-induced change in the nearby environment. Surprisingly, this effect was reversible for some molecules: a further scan some minutes later (trace e) showed that the molecule returned to the original absorption frequency. After trace g, the molecule was burned again and the whole sequence could be repeated many times.

The possibility to burn one and the same molecule several times was used to explore the kinetics of this process by measuring the "burn time" distribution.[6] By measuring a large number of burning events for one perylene molecule in the poly(ethylene) host, it was found that the various burning times are exponentially distributed, suggesting that the underlying process obeys Poisson statistics and is Markovian (Figure 7, right side). It is fairly clear that the spectral shift is caused by changes in the states of one or more TLSs coupled to the perylene electronic transition; however, the exact microscopic mechanism needs further study and may be related to the generation of molecular internal vibrational modes during fluorescence emission or to nonradiative decay of the excited state. Several single-molecule systems have shown light-induced shifting behavior, for example, terrylene in poly(ethylene)[97] and terrylene in a Shpol'skii matrix.[65] Future detailed study of such effects should shed light on the microscopic mechanisms of nonphotochemical hole burning.

In principle, single-molecule hole burning is a controllable process that could allow modification of the transition frequency of any arbitrarily chosen molecule in the polymer host. This leads naturally to the possibility of optical storage at the single-molecule level. Such an idea would require more careful control of the spectral locations of the various molecules (formatting) as well as measures to deal with the exponential waiting times. Despite these problems, optical modification of single-molecule spectra not only provides a unique window into the photophysics and low-temperature dynamics of the amorphous state, but it also allows such novel optical storage schemes to be considered.

**6. Correlation Properties of Single-Molecule Emission: Photon Antibunching.** The stream of photons emitted by a single molecule contains information about the system encoded in the arrival times of the individual photons. Figure 8a schematically shows the time-domain behavior of the photon stream for a single molecule with a dark triplet state, here taken to be pentacene. While cycling through the singlet states $S_0 \rightarrow S_1 \rightarrow S_0$, photons are emitted until intersystem crossing occurs. Since the triplet yield is 0.5%, on average 200 photons are emitted in a "bunch" before a dark period that has an average length equal to the triplet lifetime, $\tau_T$. The corresponding decay in the autocorrelation function of the emitted photons for pentacene in *p*-terphenyl is easily observed,[74] and this phenomenon has been used to measure the changes in the triplet yield and triplet lifetime from molecule to molecule that occur as a

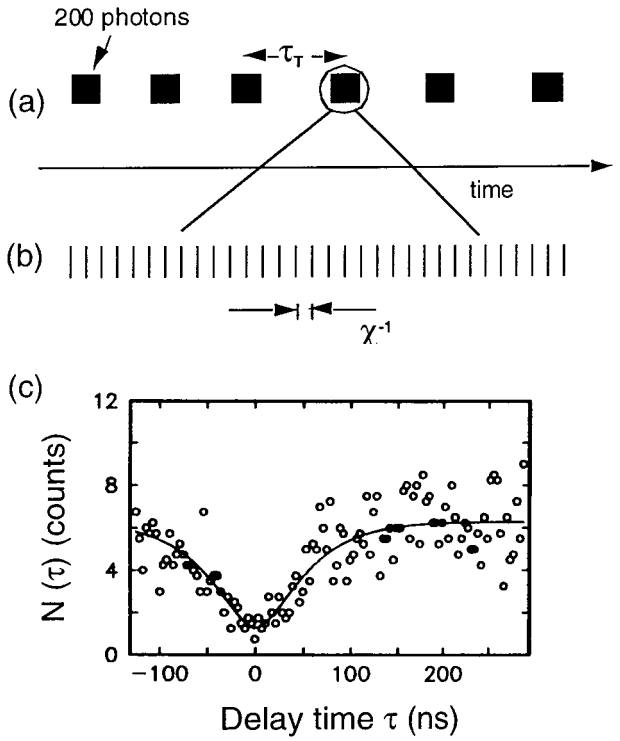


**Figure 8.** Schematic of the temporal behavior of photon emission from a single molecule showing (a) bunching on the scale of the triplet lifetime and (b) antibunching on the scale of the inverse of the Rabi frequency (middle). (c) Measured distribution of time delays between successive detected fluorescence photons for a single molecule of pentacene in *p*-terphenyl showing antibunching at $\tau = 0$. For details, see ref 9.

result of distortions of the molecule by the local nanoenvironment.[12] Such correlation measurements can also extract information on wide time scales about the spectral shifting behavior that occurs in amorphous systems[110] (*vide supra*). Although this method gives access to many decades in time, the dynamical process must be stationary, that is, the dynamics must not change during the relatively long time (many seconds) needed to record enough photon arrivals to generate a valid autocorrelation.

By contrast, in the nanosecond time regime within a single bunch (Figure 8b), the emitted photons from a single quantum system are expected to show antibunching, which means that the photons "space themselves out in time", that is, the probability for two photons to arrive at the detector at the same time is zero. This is a uniquely quantum-mechanical effect,[43] which was first observed for single Na atoms in a low-density atomic beam.[37] For a single molecule, antibunching is easy to understand as follows. After photon emission, the molecule is definitely in the ground state and cannot emit a second photon immediately. A time on the order of the inverse of the Rabi frequency must elapse before the probability of emission of a second photon is appreciable.

To observe antibunching correlations, the second-order correlation function $g^{(2)}(t)$ is generally measured by determining the distribution of time delays $N(\tau)$ between the arrival of successive photons in a dual-beam Hanbury Brown-Twiss correlator. Photon antibunching in single-molecule emission was first observed at IBM for the pentacene in *p*-terphenyl model system,[9] demonstrating that quantum optics experiments can be performed in solids and on molecules for the first time (Figure 8c). The high-contrast dip at $\tau = 0$ is strong proof that the spectral feature in resonance is indeed that of a single molecule. This observation has opened the door to a variety of other quantum-optical experiments with single molecules,[60] such as measurements of the AC-Stark shift[94] and others.[95] The convenient "trap" that the solid forms for a single molecule will allow further studies of the interactions of single molecules with the quantum radiation field.[60]

**7. Magnetic Resonance of a Single Molecular Spin.** Historically, the standard methods of electron paramagnetic resonance and nuclear magnetic resonance have been limited in sensitivity to about $10^8$ electron spins and about $10^{15}$ nuclear spins, respectively, due chiefly to the weak interaction between the individual spins and the magnetic fields used to excite the transition. The power of SMS is that only one molecule is in resonance with the laser; hence, the detection of the effect of secondary perturbing fields on the optical emission can lead to observation of weak resonances. For example, the magnetic resonance transition of a single molecular spin was first observed at IBM[39] and simultaneously at the University of Bordeaux[107] using the pentacene in *p*-terphenyl model system and a combination of SMS and optically detected magnetic resonance (ODMR). In essence, ODMR allows higher sensitivity because the weak spin transition is effectively coupled to a much stronger singlet−singlet optical transition with oscillator strength near unity. The method involves selecting a single molecule with the laser as shown in Figure 9 (left side) and monitoring the intensity of optical emission (here, fluorescence from the first excited singlet state $S_1$) as the frequency of a microwave signal is scanned over the frequency range of the triplet spin sublevels $T_x$, $T_y$, $T_z$. Since the emission rate is dependent upon the overall lifetime of the triplet (bottleneck) state, the emission rate is affected when the microwave frequency is resonant with transitions among the triplet spin sublevels.

Figure 9 (right side) shows examples of the 1480 MHz magnetic resonance transition among the $T_x-T_z$ triplet spin sublevels at 1.5 K for a single molecule of pentacene in *p*-terphenyl, where the signal plotted is the change in the fluorescence emission rate as a function of the applied microwave frequency.[39] Traces c−g show the single-molecule line shapes for four different molecules. An interesting observation is that the onset of the transition varies from molecule to molecule, in a fashion similar to the difference in onsets for the two inhomogeneously broadened site origins. The line shape of the microwave transition for a single spin is broadened by hyperfine interactions induced by the large number of different configurations possible for the nearby proton nuclear spins. This occurs because many different configurations of the proton nuclear spins in the molecule are sampled on the time scale of the measurement of the triplet state transition. In contrast, in the large *N* experiment, an ensemble average is measured rather than a time average.

These observations have opened the way for a variety of new studies of magnetic interactions in solids at the level of a single molecular spin, such as the use of external magnetic fields and deuteration to reduce proton spin flips and hence suppress the hyperfine broadening.[38] By adding radio-wave excitations, ENDOR transitions of single nuclei have also been observed.[106] In future work, the properties of amorphous organic materials may be studied in greater detail, as the selection of a single molecular spin removes all orientational anisotropy as well as all inhomogeneous broadening. Imaging on the spatial scale of a single molecule may be possible with a sufficiently large magnetic field gradient. The power of magnetic resonance in general in the study of fine and hyperfine interactions, local structure, and molecular bonding can now be enhanced with these first demonstrations of useful sensitivity in the single-

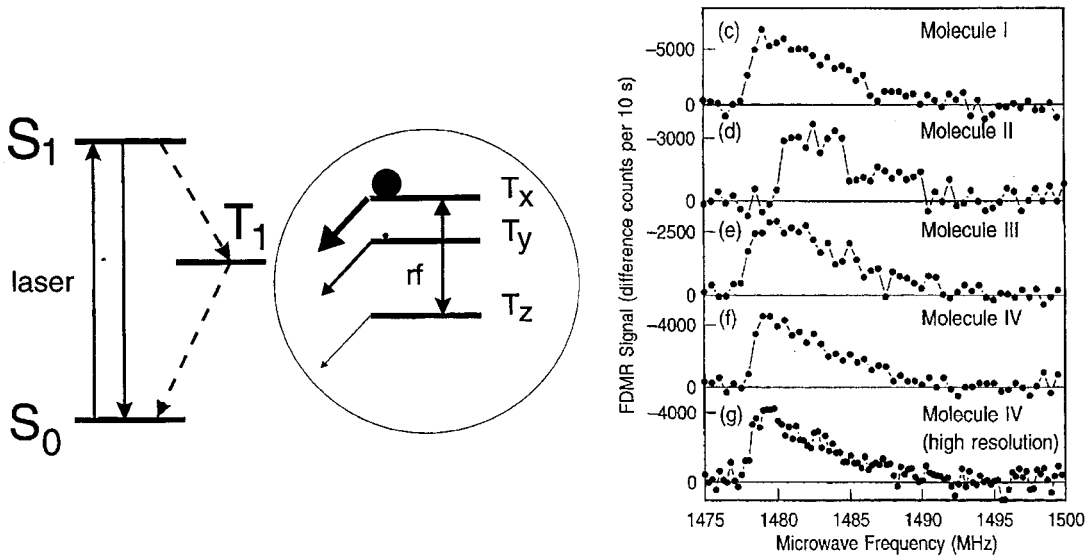


**Figure 9.** (Left) Energy levels relevant for fluorescence detected magnetic resonance of a single molecular spin. (Right) Reductions in fluorescence as a function of microwave frequency for four different single molecules of pentacene in *p*-terphenyl. For details, see ref 39.

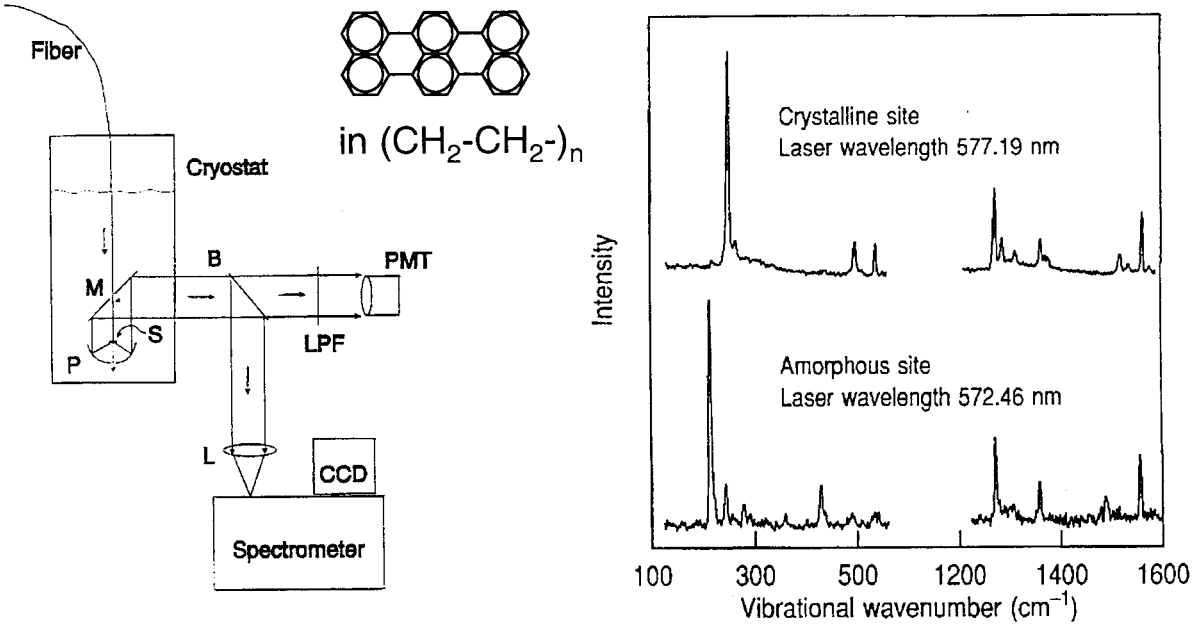


**Figure 10.** (Left) Optical configuration for exciting a single molecule at the tip of an optical fiber, collecting the fluorescence, and detecting both the spectrally dispersed emission on a CCD and the total fluorescence passing through a long-pass filter (LPF). (Right) Emission signals from two different single molecules of terrylene in poly(ethylene) at 1.6 K showing the frequencies of even vibrational modes of the ground state. For details, see ref 98.

spin regime. Some current proposals for quantum computing with spins consider small numbers (2, 3, 4,...) of carefully coupled spins, and it is possible that solid-state systems of the type described here may become useful.

**8. Vibrational Modes of Single Molecules.** The majority of SMS studies utilize the total fluorescence excitation technique where all long-wavelength-shifted photons passing through a long-pass filter are recorded. With the use of a grating spectrograph and a CCD array detector (see Figure 10, left side), vibrationally resolved emission spectra from single molecules both in crystals[96] and in polymers[98] were obtained for the first time. Such experiments may also be regarded as resonance Raman studies, since the continuous-wave laser is in resonance with the 0−0 electronic transition, and even-parity vibrational modes of the ground state are detected by measuring the shift between the laser wavelength and the wavelength of the emission peak. The ability to examine vibronic or vibrational features of individual absorbers can generate specific details about the identity of the absorber and the nature of the interactions with the nanoenvironment, producing shifts or intensity changes in the vibrational spectrum.

Figure 10, right side, shows typical dispersed fluorescence spectra for two different single molecules of terrylene in poly(ethylene) at 1.6 K. In addition to small ($\sim$cm$^{-1}$) shifts and intensity changes of various modes from molecule to molecule, two rather different classes of spectra were observed[98] as shown in the upper and lower parts of the figure. After considering various possibilities, a model was proposed in which the upper type of spectrum resulted from a terrylene molecule near or inside the crystalline region of the polymer, while the lower spectrum resulted from a single terrylene located in an amorphous region. Such results demonstrate the additional spectroscopic detail that can be obtained from individual molecules and used to probe truly local aspects of the structure of

amorphous solids. For example, the lowest frequency mode in the figure is a long-axis ring expansion of the molecule; the shift to lower energy in the amorphous site can be understood as resulting from the reduced local density (greater free volume) compared to the crystalline site. Such measurements have stimulated new theoretical calculations of the spectral changes that result from specific local distortions for comparison with the single-molecule spectra.[67]

**9. Single Molecules Interacting with Novel Optical Fields.** Two experiments have been performed in which single molecules at low temperature were probed by novel optical fields. In the first, a 60 nm diameter near-field optical probe composed of an aluminum-coated pulled optical fiber tip was used to excite single molecules of pentacene hidden below the surface of a *p*-terphenyl crystal.[66] This experiment was completed while the author was on sabbatical in the laboratory of U. P. Wild at ETH-Zürich. Single molecules within a few hundred nm of this subwavelength light source were identified either by early saturation behavior or by analysis of Stark shifts of the absorption lines produced by a static electric potential applied to the Al coating of the tip. Viewed differently, with previous measurements of Stark shift coefficients, the observed shift of the single-molecule line can be viewed as a local sensor of the highly inhomogeneous electric field of the tip.

In a second experiment, the coupling between a single molecule and the morphology-dependent resonances (MDRs) of dielectric microspheres was explored.[72] A thin sublimed crystal of *p*-terphenyl doped with pentacene and terrylene was placed in optical contact with a small microsphere, and the high-Q ($\sim 10^6$) resonances of the microsphere were excited by the evanescent field from a nearby prism. By scanning the laser frequency and detecting the emission from the sample via a low-temperature wide-field microscope, situations could be found where single-molecule absorption lines were coincident with MDRs of the sphere. Single-molecule line widths were measured in the hope of detecting an enhanced or suppressed line width signifying modifications of the spontaneous emission rate by cavity quantum electrodynamic effects. Although anomalous line widths were observed, it was not possible to conclusively assign the source to modification of the density of photon states by the MDR, due to interference from spectral diffusion effects. It remains a future research goal to couple the narrow optical absorption of a single molecule or ion trapped in a solid to a high-Q cavity in order to observe strong coupling of the molecule and the light field.

### C. Room-Temperature SMS

At room temperatures, single molecules can be observed with a variety of types of optical microscopy, including scanning near-field optical microscopy, confocal microscopy, epifluorescence, and total internal reflection microscopy. The work of the Moerner group at room temperature has concentrated on the last three methods. The pores of water-filled gels provide an aqueous environment that restricts Brownian motion so that individual molecules can be observed for extended periods. For example, these methods have been used to explore the photophysics of single copies of green fluorescent protein (GFP) mutants and other fluorescent proteins. Real-time spectral measurements yield the fluorescence resonance energy transfer characteristics of dual-GFP protein constructs designed to sense $Ca^{2+}$ ion concentrations. New understanding of the dynamical behavior of single kinesin molecular motors has been provided by polarization spectroscopy. Finally, a single molecule in a crystal can be configured to emit single photons upon demand with high probability, producing a truly quantum-mechanical light source that may be useful to cryptography. Milestones from the Moerner group are listed in Table 2, several of which will now be summarized.

**TABLE 2: Room-Temperature and Single-Biomolecule Milestones**

| experiment | refs |
|---|---|
| Diffusion of single fluorophores in poly(acrylamide) gels | 26, 41 |
| Blinking and switching of single copies of green fluorescent protein | 24, 78 |
| Imaging z-oriented molecules with total internal reflection microscopy | 25 |
| Cameleon−single-pair FRET between two GFP mutants in a [Ca++]-sensitive protein | 20 |
| *Ds*Red- a tetrameric fluorescent protein | 46 |
| Dynamics of a single-molecule pH sensor | 19 |
| Polarization analysis of kinesin motor in various nucleotide states | 91 |
| Photon antibunching for single CdSe/ZnS quantum dots | 45 |
| Single-molecule source of single photons on demand | 44 |

**1. Diffusion of Single Molecules in Gels.** For experiments hoping to obtain biologically relevant information, aqueous environments are required. Although the observation of single fluorophores diffusing through a focal volume had been accomplished by several groups by the mid-1990s, more information can be obtained when the molecules are at least partially immobilized and the same single molecule is studied for a long time. In water, a small fluorophore can move a mean-squared distance of $\sim 300\ \mu m^2$ in one second due to Brownian motion. This problem can be solved by attaching the system of interest to a surface, but this must be done carefully in order to avoid denaturation. Although useful information was obtained from dye-labeled lipids[86] in lipid bilayers and motor proteins bound on their natural counterparts,[48] it is necessary for other systems to develop appropriate immobilizing aqueous environments.

In 1996, partial immobilization of single molecules was achieved by using the water-filled pores of poly(acrylamide) gels, a technique that has been demonstrated for organic dye molecules[26] as well as for green fluorescent protein[24] (see the next section). These poly(acrylamide) gels, which are widely used for separation techniques, are not only suitable as immobilizing matrix for SMS but also can be studied themselves by using the diffusion of embedded dye molecules as a probe for the local gel environment as shown in Figure 11. The left side of the figure shows the total internal reflection (TIR) microscopy setup required for wide-field imaging. The method operates by illuminating a thin slice ($\sim$125 nm thick) of the sample with the evanescent light field produced by total internal reflection of the pumping laser beam at the interface between the upper cover slip C and the sample S. This technique has the advantage of pumping only a thin pancake-shaped volume of the aqueous sample to reduce background signals. Emission from single molecules is collected by a microscope objective MO and imaged onto a high-speed intensified CCD camera.

Excitation and detection of single nile red dye molecules in poly(acrylamide) gels by TIR microscopy allowed measurement of the three-dimensional trajectories of the spatial motion for the first time.[26] An example for the case of rhodamine 6G dye molecules in a gel[41] is shown in Figure 11, right side. For each 100 ms time step provided by the integration time of the camera, the *x* and *y* transverse position information was simply provided by the position on the two-dimensional detector (with the natural

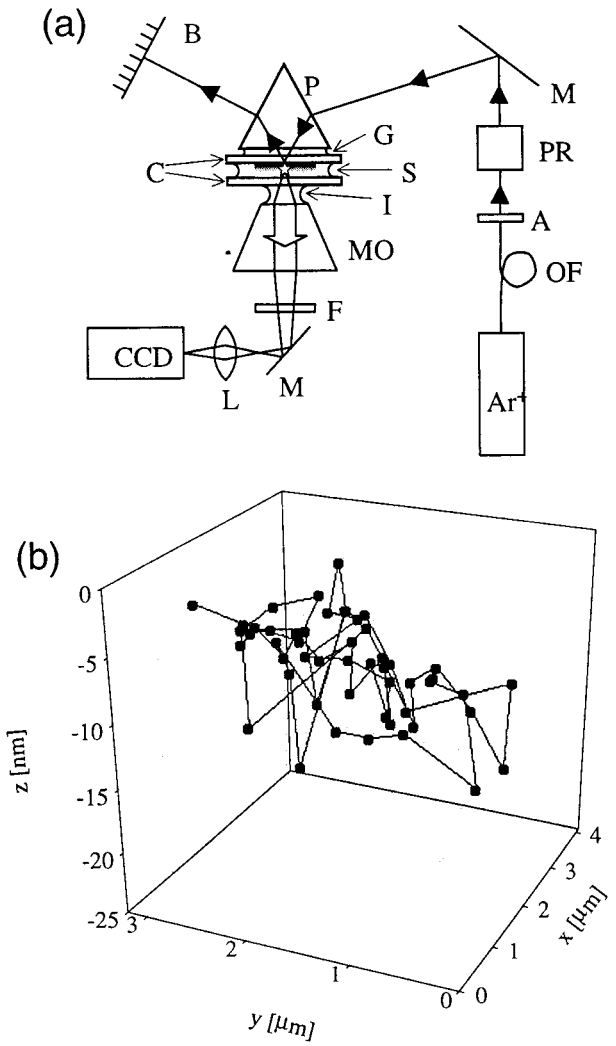


**Figure 11.** (Left) Experimental configuration for total-internal-reflection microscopy of single molecules in aqueous samples at room temperature. For details, see refs 26 and 41. (Right) Three-dimensional trajectory of a single molecule of rhodamine 6G in a poly(acrylamide) gel at room temperature, 100 ms per point. For details, see ref 41.

diffraction-limited resolution of ~200 nm). The *z* position information was obtained in a novel way: with the reasonable assumption of fast rotation of the small fluorophores in the gel, the brightness of the molecule was used to determine its axial position in the exponentially decaying evanescent field. The molecules still undergo Brownian motion, but with reduced diffusion coefficients that could be determined for various gel concentrations by analyzing the time-dependence of the mean square displacement in the $x-y$ transverse plane.[41] The cross-linked meshwork of the poly(acrylamide) gel matrix was able to decrease the diffusion coefficient for small organic dye molecules by 1 to 3 orders of magnitude, depending on the gel composition. The relation between gel concentration and diffusion coefficient confirmed estimations for the dependence of the mean pore size on concentration that were derived from molecular-sieve chromatography of proteins.[29] In more recent studies, agarose gels have also been found to be very useful for SMS, especially since no cross-linking reaction is required.

**2. Orientations of Single Molecules by Ring Patterns.** For many years, it has been well-known that useful information from the optical microscopy of specimens can be obtained by altering the polarization of the pumping light or by resolving the polarization of the emitted light. However, due to the transverse nature of a z-axis-propagating electromagnetic wave, only pump or emission components in the $x-y$ plane could be easily examined. It was demonstrated recently that the highly inhomogeneous electric field of a near-field optical tip can provide *z*-axis electric fields,[13] but this method requires specialized optical apparatus.

The use of TIR excitation to pump single molecules provides a convenient way to access optical emission dipole moments aligned along the optic (*z*) axis of the microscope. The apparatus involves using a standard oil-immersion inverted microscope to view single molecules through some thickness of water (Figure 11, left side). When imaging an aqueous sample of typical thickness of several microns with TIR, the focal plane is located at the interface between the upper cover slip and the water. However, oil-immersion objectives provide lowest aberration for focal planes located at the top of the lower cover slip. The extra propagation distance through water and the ensuing index mismatch of the water relative to glass introduce aberrations for focal planes near the upper cover slip.

This seemingly arcane fact has fascinating consequences when the emission source is a single molecule. *z*-Axis oriented molecules emit light predominantly at polar angles near $\pi/2$, and the light propagating at these high angles is aberrated the most, resulting in a ring-shaped structure at the image plane.[25] At the same time, molecules with emission dipoles in the $x-y$ plane do not show a ring structure. Due to its comparative simplicity, this technique is now being explored as to its utility in determining the three-dimensional orientation of single-molecule labels in a wide variety of biophysical situations in which oil-immersion objectives are used to observe aqueous samples.[5]

**3. Optical Study of Single Copies of the Green Fluorescent Protein and Other Fluorescent Proteins.** The green fluorescent protein (GFP) and its mutants are currently of great importance in molecular and cellular biology.[101] GFP is a small (238 amino acids), water-soluble protein isolated from the jellyfish *Aequoria victoria*, which has a $\beta$-barrel structure as shown in Figure 12a. The strongly absorbing and fluorescing chromophore of GFP located inside the barrel is formed spontaneously (in the presence of oxygen) from three amino acids in the native protein chain. No external cofactor (as in most other fluorescent proteins) is necessary. In cell biology, GFP is currently widely used as an indicator for gene expression or as a fluorescent label for a large variety of proteins. Since the quantum yield of the emission is fairly high and the absorption can be pumped by convenient Ar+ laser lines, single copies of GFP mutants may easily be observed using SMS techniques. For example, a confocal microscopy image of the "10C" mutant at low concentration in a poly(acrylamide) gel is shown in Figure 12b.[64] In this scanning method, the image is built up point by point as the small focal spot is translated over the sample, and the emission is imaged through an aperture before detection on a small-area photon counting detector.

Research in the Moerner group has yielded the first example of a room-temperature single-molecule optical switch[24] and the first details of the photophysical character of GFP on the single-copy level. By studying two different red-shifted GFP mutants (S65G/S72A/T203Y denoted "T203Y" and S65G/S72A/T203F denoted "T203F"), which differ only by the presence of a hydroxyl group near the chromophore, slight differences in the photophysical properties were observed. In particular, a fascinating and unexpected blinking behavior appeared,[24] discernible only on the single-molecule level (see the molecule at the lower edge of Figure 12b for example). This blinking behavior likely

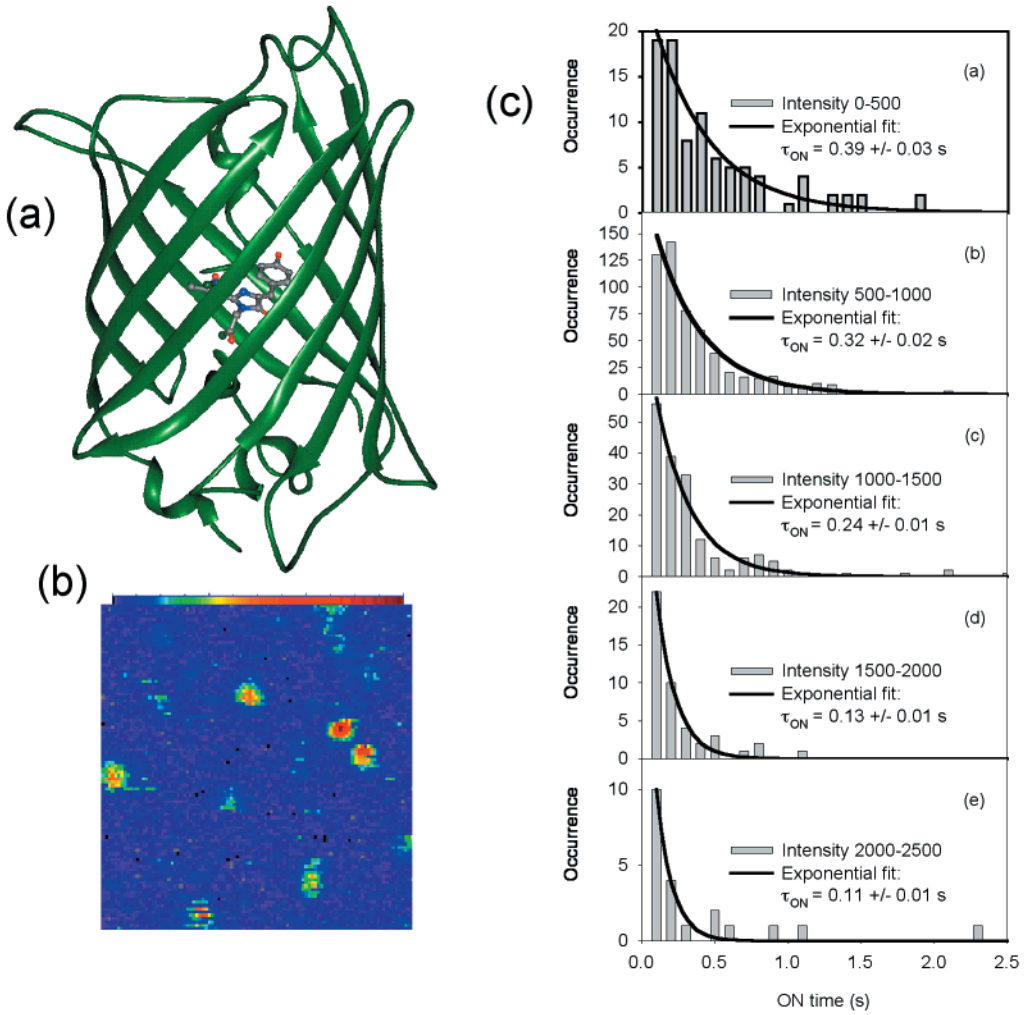


**Figure 12.** (a) Structure of the green fluorescent protein.[73] (b) Confocal fluorescence image of single copies of the mutant 10C embedded in a poly(acrylamide) matrix, 10 $\mu$m × 10 $\mu$m range, 100 points × 100 points, 10 ms counting time per point. For details, see ref 64. (c) Emission-intensity-binned histograms of the on times of the fluorescence of EGFP in agarose (pH 8) (at 488 nm excitation intensities of 5 kW/cm$^2$, 1.5 kW/cm$^2$, and 0.5 kW/cm$^2$). The molecules were binned in five emission intensity classes (intensity in arbitrary units). For details, see ref 78.

results from transformations between at least two states of the chromophore, only one of which is capable of being excited by the 488 nm pumping laser and producing fluorescence. Additionally, a much longer-lived dark state is accessible through excited state processes. Thermally stable in the dark for many minutes, this long-lived dark state can be excited at 405 nm to regenerate the original fluorescent state.

Recently these studies have been extended to other mutants of GFP ("EGFP" and "10C") and to different environments (different pH, different matrix (agarose)).[78] Rather than measuring the autocorrelation of the entire time trace, the "on-time" and "off-time" distributions were separately extracted. Mutant variation showed that the blinking behavior is very similar for all mutants studied in the phenolate ion class and is very similar in both gel hosts. Furthermore, changing the buffer pH from 6 to 10 had no effect on the on-time distributions. This observation strongly suggests that the mechanism of blinking is not proton transfer, as was suggested earlier. However, changing the excitation intensity had a strong effect on the distribution of on-times: the higher the pumping intensity, the less time the fluorescence of the molecule is on (Figure 12c). This clearly shows that the termination of the emission is photoinduced. In contrast, no evidence was found for intensity dependence of the off-times, suggesting that the conversion from the off state to the on state is spontaneous. A more likely explanation for the blinking is a reversible switching between different conformational states of the chromophore (e.g., isomerization) and/or the rest of the protein. From the single-molecule blinking experiments, the probability of termination of emission per photon absorbed was determined and found to be in agreement with the bulk bleaching quantum yield (8 ($\pm$2) × 10$^{-6}$), thus suggesting that the two processes are related. These studies, along with separate work on dynamics of the emission at shorter time scales with FCS,[87] show that the photophysical dynamics of the GFP emission are quite complex.

*Ds*Red, a tetrameric fluorescent protein cloned from the *Discosoma* genus of coral, has shown promise as a longer-wavelength substitute for green fluorescent protein (GFP) mutants for *in vivo* protein labeling. Bulk and single-molecule studies[46] of the recombinant protein revealed that the *Ds*Red chromophore shows high stability against photobleaching compared to GFP mutants. Stark modulation spectra confirm that the electronic structure of the *Ds*Red chromophore is similar to that for GFP. However, the tetrameric nature of *Ds*Red leads to intersubunit energy transfer, as evidenced by the molecule's unusually low anisotropy (0.23 $\pm$ 0.02). This value is approximately consistent with an estimate of the energy transfer rates between the monomeric units based on crystallographic information. The fluorescence emission bleaches at a rate that is linear in the applied excitation intensity, implying that the

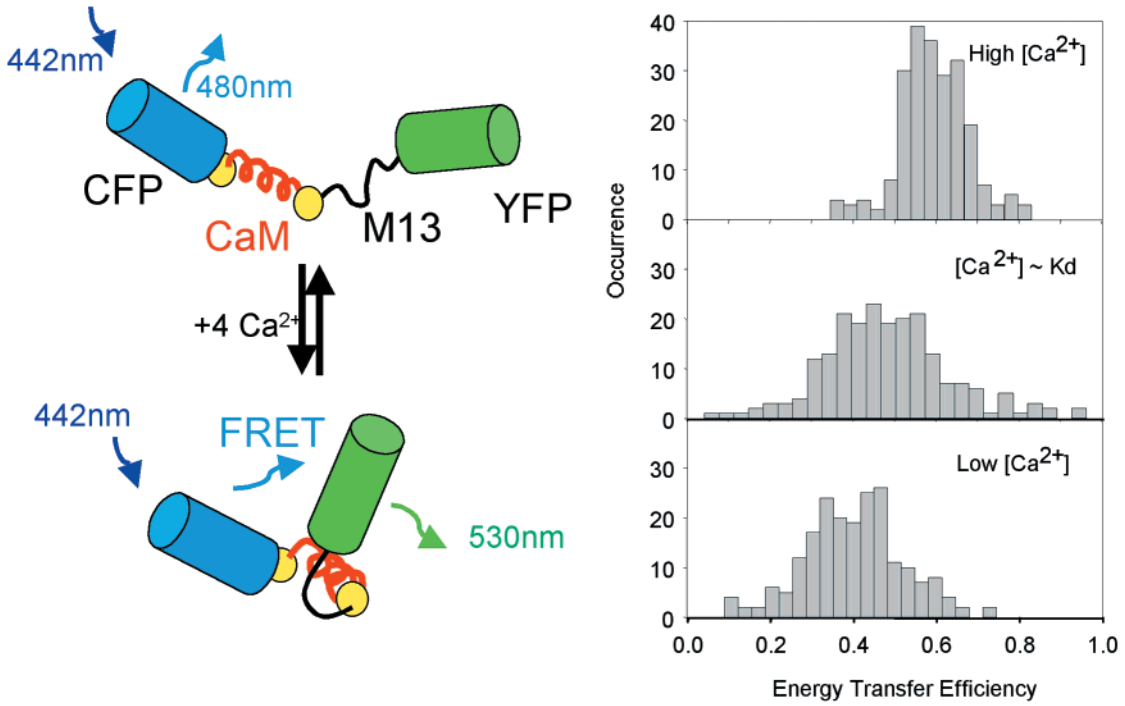


**Figure 13.** (Left) Schematic of the structure of cameleon and the change in FRET upon binding and unbinding of $Ca^{2+}$ ions. (Right) Histograms of the energy transfer efficiency measured for single molecules of cameleon in agarose gels, at three different $Ca^{2+}$ ion concentrations. For details, see ref 20.

dark states are photochemically created and, consistent with the tetrameric structure, several photobleaching "steps" were observed during the decay of individual complexes. Because approximately a factor of 10 more photons are emitted before bleaching, this study suggests that *Ds*Red may be superior to some GFP-based labeling technologies as long as tetramerization is not an issue.

Happily, the search still continues for improved genetically encoded fluorescent proteins that reach the level of photostability shown by laser-dye fluorophores such as rhodamines and cyanine dyes. When such labels are available, the applications of fluorescent protein mutants to single-molecule studies will increase even further.

**4. Single-Molecule Concentration Sensors.** SMS can be used to explore the dynamics of environment-dependent fluorescent molecules that are conventionally employed as concentration reporters in biological systems. One study in the Moerner laboratory concerned the "cameleon YC2.1" complex, whose structure is based on a cyan-emitting GFP (CFP) separated from a yellow-emitting GFP (YFP) by the calmodulin $Ca^{2+}$-binding protein and a calmodulin-binding peptide (M13) (see Figure 13, left side). This complex was designed by A. Miyawaki and R. Y. Tsien to allow sensing of calcium concentration in cells by fluorescence resonant energy transfer (FRET). If $Ca^{2+}$ ions are bound, the construct forms a more compact shape, leading to a higher efficiency of excitation transfer from the donor CFP to the acceptor YFP. The degree of FRET in cameleon is therefore a sensitive ratiometric reporter of the concentration of $Ca^{2+}$ in solution and cells.[49]

Analysis of single-molecule signals from the cameleon YC2.1 complex diluted in aqueous agarose gels allowed retrieval of several interesting features of the energy transfer between the donor and acceptor mutants of the construct, as a function of the calcium concentration in the medium.[20] The energy transfer efficiency distribution deduced from single-molecule confocal fluorescence signals shows an increased width at the $Ca^{2+}$ dissociation constant concentration (Figure 13, right side). This observation is consistent with the ligand binding kinetics, whose time scale at intermediate calcium concentration is close to our measurement time scale (20−200 ms). The complex dynamics of the fluctuations were examined using a combination of autocorrelation and cross-correlation in conjunction with polarization measurements. Beside reorientation fluctuations of the two dipoles that seem to occur slowly compared to the emission time scale but fast compared to the integration time, slower variations in the energy transfer between the two GFP mutants were observed. Both negative and positive cross-correlations in the donor and acceptor emission signals were present, the former related to the energy transfer process, and the latter caused by other perturbations of the donor and acceptor emission.

In separate measurements, the pH-sensitive fluorescent reporter molecule Dextran-SNARF-1 (Molecular Probes, Eugene, OR) was explored at the single-copy level by confocal fluorescence microscopy.[19] A variation of the pH in the aqueous solution induces a change of the ratio between the emission intensities at 580 and 640 nm, with much faster binding kinetics than the measurement time scale. The distribution of this ratio measured on single copies of this chromophore immobilized in agarose showed, however, an increased width close to the p$K_a$. Because the binding kinetics are fast, inhomogeneities in either the Dextran or in the gel environment may be responsible for this observation.

**5. Kinesin Motor Proteins: Orientational Flexibility as a Function of Nucelotide Bound.** A key scientific problem for a number of investigators continues to be to understand the molecular mechanisms of mechanochemical force transduction by motor proteins. Through a collaboration with the laboratory of Prof. L. S. B. Goldstein, UCSD, we have recently utilized single- and multiple-molecule methods to explore the eukaryotic motor protein, kinesin, which is known to processively "walk" along microtubules to carry cellular cargo. Previous motility analyses using laser traps suggested that kinesin takes 8 nm steps for every ATP hydrolyzed.[93,102] On the other hand, the

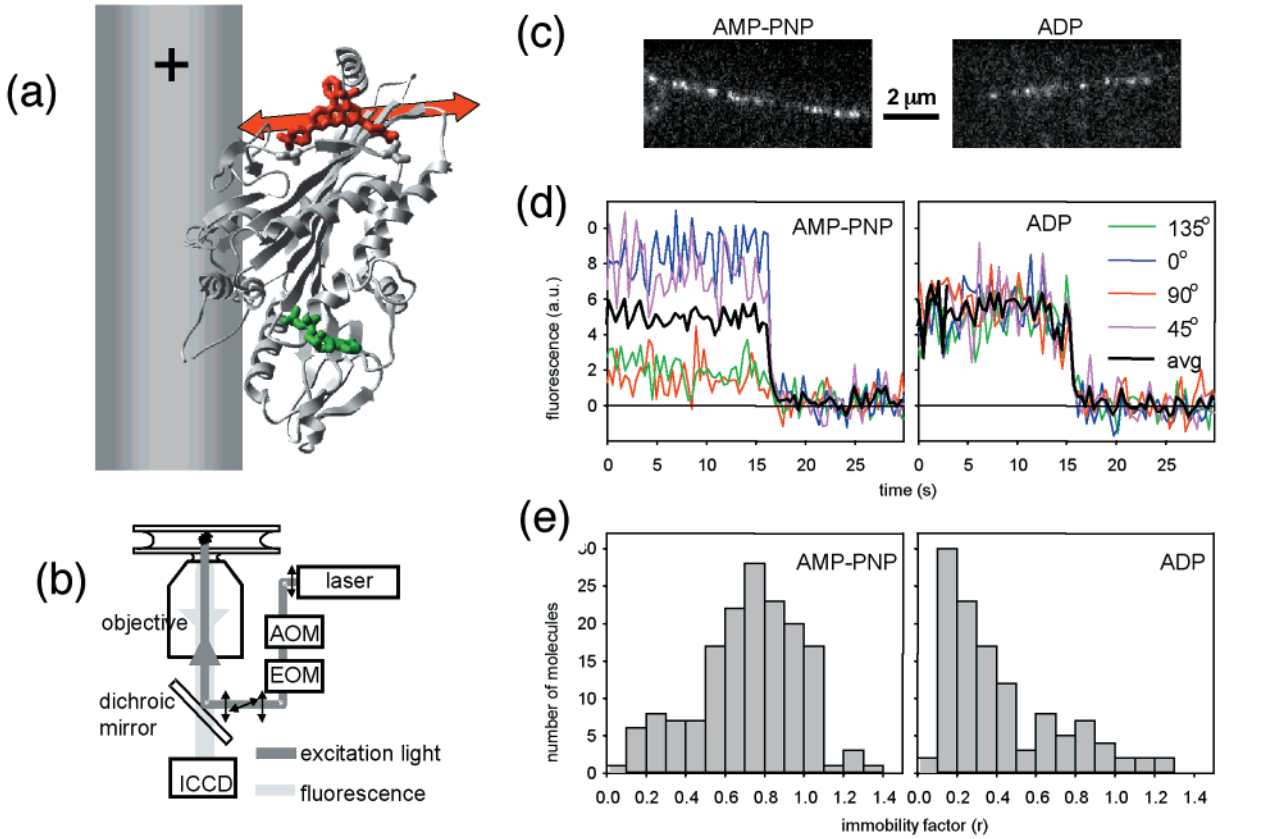


**Figure 14.** Polarization microscopy of single kinesin motor proteins. (a) Model of kinesin head and its orientation while bound to the microtubule. (b) Experimental apparatus for measuring linear dichroism by polarization microscopy. (c) Single kinesin heads bound to a microtubule in the presence of AMP−PNP and ADP. (d) Emission signals from a single molecule for four different pumping polarizations as a function of time. The single molecule bleached at 17 s in the left panel and at 15 s in the right panel. (e) Immobility factor distribution for single molecules. For details, see ref 91.

X-ray and electron microscope structural data fail to reveal any bond conformation of the two heads of the kinesin molecule that can span the required 8 nm distance. This and other mysteries relating to exactly how kinesin works formed the primary motivation for the experiments.

To explore the orientational mobility of single kinesin heads as a function of nucleotide bound, a careful protocol was devised for the covalent attachment of a single fluorescent label to a well-defined position on the surface of the protein.[91] Using a model X-ray structure and information from cryoelectron microscopy, Figure 14a illustrates the relative positions of the kinesin motor protein head and the microtubule, with the nucleotide binding site shown in green, the fluorescent rhodamine label in red, and the orientation of the absorption dipole of the fluorophore shown as a red arrow (see ref 91 for details). A key aspect of these experiments was the use of a doubly attached fluorescent reporter molecule. To have the fluorophore provide a faithful representation of the orientation of the enzyme, a kinesin mutant was prepared with a properly spaced pair of cysteine residues, and a bifunctional iodoacetamide derivative of rhodamine was bound to the two cysteine residues. To simplify the situation, a monomeric form of kinesin was used, and this construct was provided with one of four possible analogues of the nucleotide to mimic four stages in the hydrolysis of ATP: no nucleotide, AMP−PNP mimicking ATP, ADP−$AlF_4^-$ mimicking ADP−Pi, and ADP.

The experimental apparatus (Figure 14b) utilized a wide-field, epifluorescence polarization spectroscopy microscope with single-molecule sensitivity and 100 ms time resolution. The sample consisted of axonemal microtubules in buffer stuck to the lower cover slip to which kinesin heads were bound. Modulation of the polarization of the pumping light allowed sensing of the orientation of the absorption dipoles as a function of time and nucleotide state. By recording images of the emission from the sample with an intensified CCD camera in synchrony with the pumping modulation, the linear dichroism of the sample could be measured.

Ensemble measurements of the linear dichroism for kinesin monomers as a function of nucleotide state revealed a surprise. While three of the nucleotide states revealed clear, well-defined orientations of the kinesin heads, surprisingly in the ADP state, the measured linear dichroism values were close to zero. This interesting result had three possible interpretations: (a) the transition dipole axial angle with respect to the axoneme had become the magic angle, 54.7 degrees, (b) the dipoles were statically disordered, with different axial angles from kinesin head to kinesin head, or (c) the dipoles were dynamically disordered on the 100 ms time scale of the measurements. These three possibilities cannot be distinguished with traditional ensemble measurements.

Single-molecule measurements have provided an elegant solution to this problem, because by observing the kinesin heads, one at a time, these three possible explanations can be distinguished. As shown in Figure 14c for both AMP−PNP and ADP states, single kinesin heads can be observed bound to the axoneme (the row of bright spots shows the location of the axoneme). Of course, single-molecule experiments often produce extra information and require improved methods of data analysis. The goal of this measurement is to learn more about the axial angle of the molecular dipole with respect to the long axis of

the microtubule. First, it is necessary to recall that the optical measurements sense the function $|\vec{\mu}\cdot\vec{E}|^2$. This function does not immediately tell the direction of the absorption dipole $\vec{\mu}$ with respect to the direction of the laser electric field $\vec{E}$. In addition, single kinesin motors have not only a projection along the axonemal microtubule but there is also an azimuthal angle of the absorption dipole around the circumference of the microtubule, which varies from single molecule to single molecule.

To extract orientational data, the single-molecule images were recorded for four pumping polarizations: 0, 45, 90, and 135 degrees in the plane of the microscope. Figure 14d shows time trajectories of the emission from a single molecule with AMP−PNP bound (left) and with ADP bound (right). For AMP−PMP, the projections of the absorption dipole along the four pumping directions are different, which shows that the head has a well-defined static orientation in agreement with the earlier ensemble data. For ADP bound, surprisingly, the projections of the absorption dipole along the four pumping polarizations are all equal! This shows that the dipole is dynamically disordered on the time scale of the measurement (100 ms), which is case (c) above. A further enhancement to the analysis of the single-molecule data involves definition of an immobility parameter, *r*. Small values of *r* correspond to large cone angles, while *r* values near 1 signify a fixed dipole orientation. Figure 14e shows histograms of the distribution of *r* values for single kinesin motors. Clearly the cone angle is small for AMP−PNP but very large for ADP. The full details may be found in ref 91.

Several conclusions may be extracted from this study. The kinesin head maintains a rigid orientation in the presence of analogues of the ATP, ADP−Pi, or no nucleotide states. Surprisingly, in the presence of ADP, the motor domain of kinesin, while still bound to the microtubule, adopts a novel and previously undescribed highly mobile rocking state. This state may be a general feature in the chemomechanical cycle of motor proteins; in the case of kinesin the transition to a rigid state after ADP release may contribute to the generation of the 8 nm step. In addition, the flexibility of the bound head for ADP may allow the conventional dimeric kinesin to span the required 8 nm while still maintaining both heads bound to the microtubule. This experiment is an important example of the particular ability of single-molecule optical investigations to provide new information of biological relevance that cannot be obtained by conventional ensemble-averaged techniques. In future work, the orientational changes that occur when dimeric kinesin walks along microtubules will be interesting to observe.

**6. Room-Temperature Quantum Optics: Antibunching for Single Quantum Dots and a Source of Single Photons Utilizing a Single-Molecule Emitter.** The earlier observations of photon antibunching for a single molecule in a solid at low temperatures described in section A.6 above provided the first example of this quantum optical effect for a molecule and for a solid host, as opposed to earlier work with an atomic beam or a single ion in a trap. In the years since, several groups have worked to extend single-molecule quantum optics to the room-temperature regime. One type of room-temperature single-quantum system recently addressed by the Moerner group has been single semiconductor nanocrystals.[1,70] Single semiconductor nanocrystals (also called quantum dots) have been proposed for fluorescent labels for biological applications. It is well known that such nanocrystals blink and fluctuate on time scales from microseconds to many seconds,[42] a property that may limit their applicability for sensitive fluorescence applications.

To complement earlier studies of the blinking and fluctuations at long times, we have investigated the optical emission dynamics of single nanocrystals on the short (ns) time scale of the excited-state lifetime in collaboration with the laboratory of P. Alivisatos.[45] The fluorescence intensity correlation function of a single CdSe/ZnS quantum dot can be obtained via confocal microscopy using a start−stop experiment, that is, detection of the time delay between pairs of emitted photons with a Hanbury Brown-Twiss correlator. Such an experiment senses how well the nanocrystal emission resembles that for a simple two-level system, and in particular if biexcitonic emission can occur. We observed for the first time strong photon antibunching in a single quantum dot, a signature of nonclassical light emission, over a large range of intensities (0.1−100 kW/cm$^2$). The lack of coincidence events at zero time delay even at higher intensities indicates the presence of a highly efficient Auger ionization process, which suppresses multiphoton emission in these colloidal quantum dots. Using careful analysis of the saturation behavior of the coincidence histograms, the absorption cross section of a single quantum dot has also been determined. Thus, despite the blinking and fluctuation effects that occur at long times, at short times the quantum dot behaves as a simple two-level system. If the long-time effects can be reduced, these quantum dots may indeed be useful as fluorescent reporters.

To perform quantum optical experiments on a single small fluorophore, a highly stable single molecule is required. In recent years, researchers have shown that terrylene molecules protected from photooxidation in a *p*-terphenyl crystal at room temperature show a very low probability of photobleaching,[40] and this system was recently utilized to produce an optical source of single photons on demand in collaboration with B. Lounis.[44] A high-performance, room-temperature source of single photons upon demand would be a key component in an optical quantum cryptography and communication system. Encoding of information in entangled polarization states achieves the highest level of reliability when single photons, one at a time, are used. More than one photon present during each clock cycle would be vulnerable to eavesdropping by a so-called beam splitter attack, because the loss of the extra photons might not be detected.

The key idea for producing a source of single photons using a single molecule is shown in Figure 15a. The emission from a thin crystal of *p*-terphenyl doped with an extremely low concentration of terrylene molecules can be obtained by standard confocal microscopy in an inverted microscope as shown in the image in the center of the figure. The focal spot is placed so as to pump only one of the molecules, and the pumping radiation consists of a short 35 ps laser pulse from a mode-locked laser at 532 nm. If this is done properly (see the approximate level diagram in Figure 15b), the molecule can be placed in the excited emitting state with high probability by each pump pulse. More precisely, if the pulse energy is high enough, pumping into a vibronic sideband of the electronic excited state uses the short lifetime of the vibronic level compared to the relatively long lifetime of the lowest electronic excited state to populate the latter efficiently. (This method of achieving inversion is simpler than using a $\pi$-pulse.) Because the fluorescence quantum yield is high, the molecule then emits one and only one fluorescent photon for each pump pulse.

The observed performance of the single molecule as a single photon source was quite good. By determining the overall rate of photon emission and comparing this to the pumping rate provided by the pulsed laser, the probability of single-photon events could be determined. The (source) probability of generation of a single photon per pulse, $p(1)$, was very large (86%), while $p(0)$ is approximately $[1 - p(1)]$ (14%), and $p(n > 1) \sim 0$. Clearly, this distribution is highly non-Poissonian. The ratio

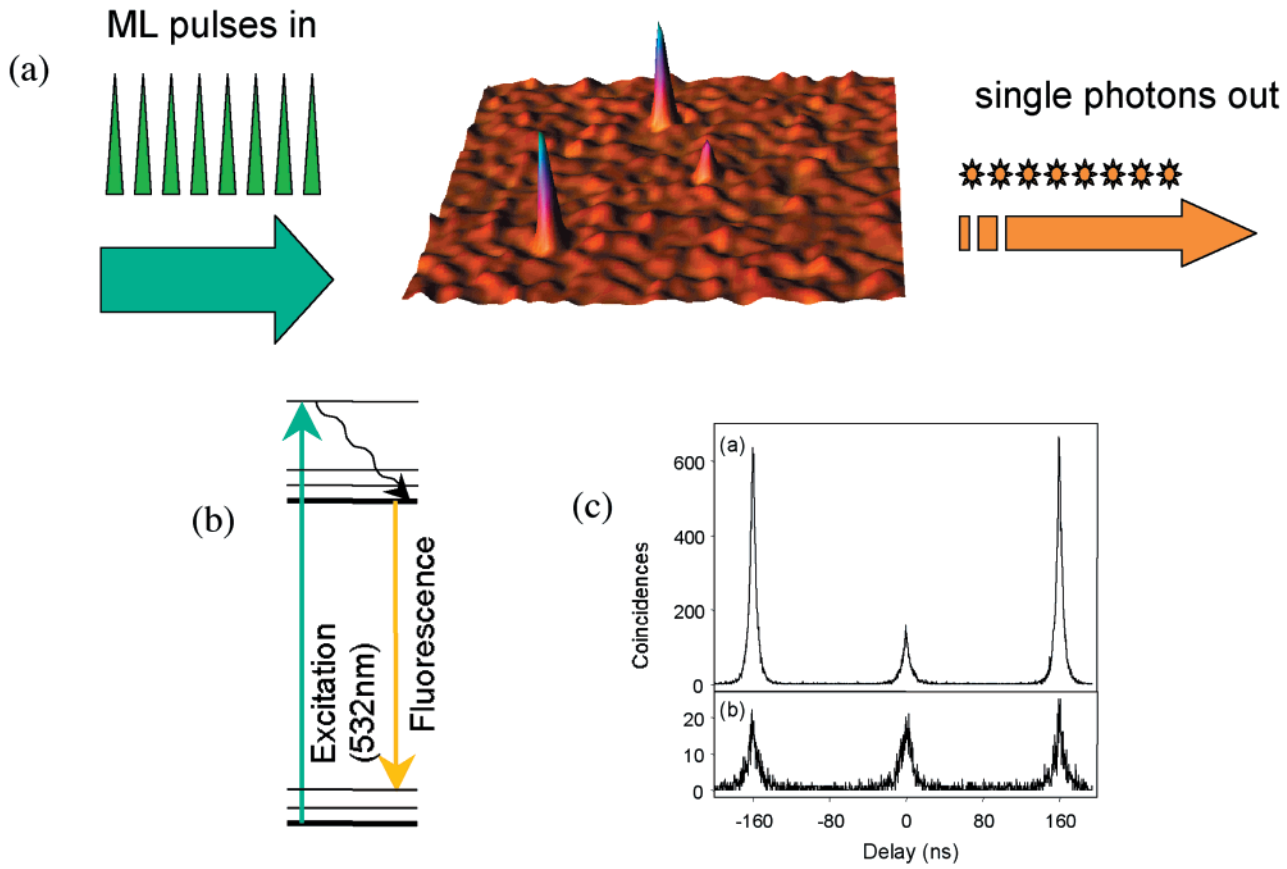


**Figure 15.** Scheme of the single photon source based on a single molecule. (a) overall idea of the method. The confocal image shows the locations of single molecules of terrylene in a crystal of *p*-terphenyl at room temperature. Mode-locked (ML) laser pulses 35 ps in length pump the sample, and the single molecule can be made to emit one photon with high probability for each pump pulse. (b) Approximate level scheme for terrylene, showing pumping into vibronic sidebands but emission from the lowest singlet state. (c) Second-order correlation function for the emitted photons: upper panel for the single-molecule emission, lower panel for the background emission from the sample. For details, see ref 44.

of $p(1)$ to $p(0)$ was far larger than for other sources of single photons based on low temperature techniques. In addition, measurement of the intensity correlation of the emitted light (Figure 15c) confirmed the highly quantum-mechanical nature of the emission. In the lower panel, the laser spot is placed away from a molecule, and the detected background photons show equal-amplitude peaks every 160 ns due to the repetition rate of the laser. However, when the laser spot is placed on the single molecule (upper panel), the central peak is far smaller than the two side peaks, a signature of the quantum mechanical character of the emitted photons. In fact, the central peak can be reduced even further by trivially reducing the concentration of out-of-focus molecules. In summary, this method for producing a source of single photons at room temperature not only shows high performance but it is also quite simple and easy to implement with a confocal microscope and a pulsed laser source. To be able to use this for a real application, however, the emitted photons must be collected with high efficiency, perhaps by coupling the single-molecule emitter to a resonant cavity.

### D. Summary

The research described here shows how the high signal-to-noise ratios now available in optical single-molecule measurements allow for a wide variety of experiments in many fields. In all cases, the main benefit of single-molecule isolation is the unraveling of ensemble averages. New insight is thus gained into the structure and dynamics of condensed or living matter at nanometer scales, not only when inhomogeneities cause different molecules to behave in wildly different ways but also for identical nanosystems that fluctuate in time. Whereas time-resolved measurements on an ensemble demand synchronization of all subsystems, single-molecule experiments yield time-resolved information automatically.

The impact of single-molecule spectroscopy has been felt in physics and chemistry, and the application to biological problems is currently under intense development. In the area of physical chemistry, single molecules at low temperatures have provided a wealth of new information about such fundamental processes as tunneling and activation in molecular crystals and polymers. Single molecules will also help solve problems in physical chemistry at ambient conditions, such as surface-enhanced Raman scattering, nanocrystal photophysics,[71] adsorption and desorption of molecules on surfaces, and dynamics in polymers and in other complex environments. The scope and potential of single-molecule methods in biology are quite broad, as both molecular heterogeneity and single-molecule operations are characteristic of biomolecular systems. The domains of biophysical chemistry that could benefit from single-molecule investigations range from protein folding and colocalization to the interaction between single biomacromolecules, from the mechanisms of molecular motors to the sequencing of single nucleic acid strands. A key area of current interest involves development of methods to observe single molecules in living cells. In collaboration with the group of H. McConnell, we have recently been able to detect single copies of major histocompatibility complex type II (MHC II) proteins diffusing in the

membranes of live cells.[103] Finally, much work in modern science concerns manipulation of atoms and molecules at the nanoscale, with one long-term goal being the actual production of man-made molecular-scale devices and computing machines at some time in the future. Optical probing of single molecules may be a natural readout scheme that may be useful when interconnection problems and density issues prevent conventional wiring.

**Acknowledgment.** Portions of this article have been based on an article by W. E. Moerner in *Single Molecule Spectroscopy*; Rigler, R., Orrit, M., Basche, T., Eds. (Springer-Verlag: Heidelberg-New York, 2002). The author warmly thanks many members of the Moerner single-molecule spectroscopy group for their crucial contributions to the work reported here, in particular: T. P. Carter, L. Kador, W. P. Ambrose, Th. Basché, P. Tchénio, J. Köhler, D. J. Norris, R. M. Dickson, S. Kummer, E. J. G. Peterman, S. Brasselet, H. Sosa, J. Deich, and B. Lounis. Stimulating collaborations with A. B. Myers, J. Schmidt, M. Orrit, U. P. Wild, L. S. B. Goldstein, P. Alivisatos, and S. G. Boxer are gratefully acknowledged. This work has been supported in part by grants in the late 1980s and early 1990s from the U.S. Office of Naval Research, by the National Science Foundation grant nos. DMR-9612252 and MCB-9816947, and by support from the IBM Research Division, the University of California San Diego, and Stanford University.

## References and Notes

(1) Alivisatos, P. *Mater. Res. Soc. Bull.* **1995**, *20*, 23−32.
(2) Ambrose, W. P.; Basché, T.; Moerner, W. E. *J. Chem. Phys.* **1991**, *95*, 7150.
(3) Ambrose, W. P.; Goodwin, P. M.; Jett, J. H.; VanOrden, A.; Werner, J. H.; Keller, R. A. *Chem. Rev.* **1999**, *99*, 2929−2956.
(4) Ambrose, W. P.; Moerner, W. E. *Nature* **1991**, *349*, 225.
(5) Bartko, A. P.; Dickson, R. M. *J. Phys. Chem. B* **1999**, *103*, 11237−11241.
(6) Basché, T.; Ambrose, W. P.; Moerner, W. E. *J. Opt. Soc. Am. B* **1992**, *9*, 829.
(7) Basché, T.; Kummer, S.; Bräuchle, C. *Nature* **1995**, *373*, 132−134.
(8) Basché, T.; Moerner, W. E. *Nature* **1992**, *355*, 335.
(9) Basché, T.; Moerner, W. E.; Orrit, M.; Talon, H. *Phys. Rev. Lett.* **1992**, *69*, 1516−1519.
(10) *Single Molecule Optical Detection, Imaging, and Spectroscopy*; Basché, T., Moerner, W. E., Orrit, M., Wild, U. P., Eds.; Verlag-Chemie: Munich, 1997.
(11) Bergquist, J. C.; Hulet, R. G.; Itano, W. M.; Wineland, D. J. *Phys. Rev. Lett.* **1986**, *57*, 1699−1702.
(12) Bernard, J.; Fleury, L.; Talon, H.; Orrit, M. *J. Chem. Phys.* **1993**, *98*, 850.
(13) Betzig, E.; Chichester, R. J. *Science* **1993**, *262*, 1422−28.
(14) Binnig, G.; Quate, C. F.; Gerber, C. *Phys. Rev. Lett.* **1986**, *56*, 930.
(15) Binnig, G.; Rohrer, H. *Rev. Mod. Phys.* **1987**, *59*, 615.
(16) Bjorklund, G. C. *Opt. Lett.* **1980**, *5*, 15.
(17) Bjorklund, G. C.; Levenson, M. D.; Lenth, W.; Ortiz, C. *Appl. Phys. B* **1983**, *32*, 145.
(18) Block, S. M. *Cell* **1998**, *93*, 5−8.
(19) Brasselet, S.; Moerner, W. E. *Single Molecules* **2000**, *1*, 15−21.
(20) Brasselet, S.; Peterman, E. J. G.; Miyawaki, A.; Moerner, W. E. *J. Phys. Chem. B* **2000**, *104*, 3676−3682.
(21) Carter, T. P.; Manavi, M.; Moerner, W. E. *J. Chem. Phys.* **1988**, *89*, 1768.
(22) de Vries, H.; Wiersma, D. A. *J. Chem. Phys.* **1979**, *70*, 5807.
(23) Dehmelt, H.; Paul, W.; Ramsey, N. F. *Rev. Mod. Phys.* **1990**, *2*, 525.
(24) Dickson, R. M.; Cubitt, A. B.; Tsien, R. Y.; Moerner, W. E. *Nature* **1997**, *388*, 355−358.
(25) Dickson, R. M.; Norris, D. J.; Moerner, W. E. *Phys. Rev. Lett.* **1998**, *81*, 5322−5325.
(26) Dickson, R. M.; Norris, D. J.; Tzeng, Y.-L.; Moerner, W. E. *Science* **1996**, *274*, 966−69.
(27) Diedrich, F.; Krause, J.; Rempe, G.; Scully, M. O.; Walther, H. *IEEE J. Quantum Elect.* **1988**, *24*, 1314.
(28) Eigen, M.; Rigler, R. *Proc. Natl. Acad. Sci. U.S.A.* **1994**, *91*, 5740−5747.
(29) Fawcett, J. S.; Morris, C. J. O. R. *Sep. Sci.* **1966**, *1*, 9−26.
(30) Friedrich, J.; Haarer, D. In *Optical Spectroscopy of Glasses*; Zschokke, I., Ed.; Reidel: Dordrecht, 1986; p 149.
(31) Geva, E.; Skinner, J. L. *J. Phys. Chem. B* **1997**, *101*, 8920−8932.
(32) Güttler, F.; Irngartinger, T.; Plakhotnik, T.; Renn, A.; Wild, U. P. *Chem. Phys. Lett.* **1994**, *217*, 393.
(33) Ha, T.; Laurence, T. A.; Chemla, D. S.; Weiss, S. *J. Phys. Chem. B* **1999**, *103*, 6839−6850.
(34) Itano, W. M.; Bergquist, J. C.; Wineland, D. J. *Science* **1987**, *237*, 612.
(35) Kador, L.; Horne, D. E.; Moerner, W. E. *J. Phys. Chem.* **1990**, *94*, 1237−1248.
(36) Kador, L.; Latychevskaia, T.; Renn, A.; Wild, U. P. *J. Chem. Phys.* **1999**, *111*, 8755−8758.
(37) Kimble, H. J.; Dagenais, M.; Mandel, L. *Phys. Rev. Lett.* **1977**, *39*, 691.
(38) Köhler, J.; Brouwer, A. C. J.; Groenen, E. J. J.; Schmidt, J. *Science* **1995**, *268*, 1457−1460.
(39) Köhler, J.; Disselhorst, J. A. J. M.; Donckers, M. C. J. M.; Groenen, E. J. J.; Schmidt, J.; Moerner, W. E. *Nature* **1993**, *363*, 242−244.
(40) Kulzer, F.; Koberling, F.; Christ, T.; Mews, A.; Basche, T. *Chem. Phys.* **1999**, *247*, 23−34.
(41) Kummer, S.; Dickson, R. M.; Moerner, W. E. *Proc. Soc. Photo-Opt. Instrum. Eng.* **1998**, *3273*, 165−173.
(42) Kuno, M.; Fromm, D. P.; Hamann, H. F.; Gallagher, A.; Nesbitt, D. J. *J. Chem. Phys.* **2000**, *112*, 3117−3120.
(43) Loudon, R. *The Quantum Theory of Light*, 2nd ed.; Clarendon: Oxford, 1983.
(44) Lounis, B.; Moerner, W. E. *Nature* **2000**, *407*, 491−493.
(45) Lounis, B. L.; Bechtel, H. A.; Gerion, D.; Alivisatos, P.; Moerner, W. E. *Chem. Phys. Lett.* **2000**, *329*, 399−404.
(46) Lounis, B. L.; Deich, J.; Rosell, F. I.; Boxer, S. G.; Moerner, W. E. *J. Phys. Chem. B* **2001**, *105*, 5048−5054.
(47) Magde, D. L.; Elson, E. L.; Webb, W. W. *Biopolymers* **1974**, *13*, 29.
(48) Mehta, A. D.; Reif, M.; Spudich, J. A.; Smith, D. A.; Simmons, R. M. *Science* **1999**, *283*, 1689−1695.
(49) Miyawaki, A.; Llopis, J.; Heim, R.; McCaffrey, J. M.; Adams, J. A.; Ikura, M.; Tsien, R. Y. *Nature* **1997**, *388*, 882.
(50) *Persistent Spectral Hole-Burning: Science and Applications*; Moerner, W. E., Ed.; Springer: Berlin, 1988.
(51) Moerner, W. E. Persistent Spectral Hole-Burning: Photon-Gating and Fundamental Statistical Limits. In *Polymers for Microelectronics, Science, and Technology*; Tabata, Y., Mita, I., Nonogaki, S., Eds.; Kodansha Scientific: Tokyo, 1990.
(52) Moerner, W. E. *New J. Chem.* **1991**, *15*, 199−208.
(53) Moerner, W. E. *Science* **1994**, *265*, 46−53.
(54) Moerner, W. E. *J. Lumin.* **1994**, *60*(1), 997−1002.
(55) Moerner, W. E. *Acc. Chem. Res.* **1996**, *29*, 563.
(56) Moerner, W. E. *Science* **1997**, *277*, 1059.
(57) Moerner, W. E.; Ambrose, W. P. *Phys. Rev. Lett.* **1991**, *66*, 1376.
(58) Moerner, W. E.; Basché, T. *Angew. Chem., Int. Ed. Engl.* **1993**, *32*, 457.
(59) Moerner, W. E.; Carter, T. P. *Phys. Rev. Lett.* **1987**, *59*, 2705.
(60) Moerner, W. E.; Dickson, R. M.; Norris, D. J. *Adv. Atom. Mol. Opt. Phys.* **1997**, *38*, 193−236.
(61) Moerner, W. E.; Kador, L. *Anal. Chem.* **1989**, *61*(1), A1217−A1223.
(62) Moerner, W. E.; Kador, L. *Phys. Rev. Lett.* **1989**, *62*, 2535−38.
(63) Moerner, W. E.; Orrit, M. *Science* **1999**, *283*, 1670−1676.
(64) Moerner, W. E.; Peterman, E. J. P.; Brasselet, S.; Kummer, S.; Dickson, R. M. *Cytometry* **1999**, *36*, 232−238.
(65) Moerner, W. E.; Plakhotnik, T.; Irngartinger, T.; Croci, M.; Palm, V.; Wild, U. P. *J. Phys. Chem.* **1994**, *98*, 7382−89.
(66) Moerner, W. E.; Plakhotnik, T.; Irngartinger, T.; Wild, U. P.; Pohl, D.; Hecht, B. *Phys. Rev. Lett.* **1994**, *73*, 2764.
(67) Myers, A. B.; Tchénio, P.; Zgierski, M.; Moerner, W. E. *J. Phys. Chem.* **1994**, *98*, 10377.
(68) Nie, S.; Chiu, D. T.; Zare, R. N. *Science* **1994**, *266*, 1018−21.
(69) Nie, S.; Zare, R. N. *Annu. Rev. Biophys. Biomol. Struct.* **1997**, *26*, 567−96.
(70) Nirmal, M.; Brus, L. *Acc. Chem. Res.* **1999**, *32*, 407−414.
(71) Nirmal, M.; Dabbousi, B. O.; Bawendi, M. G.; Macklin, J. J.; Trautman, J. K.; Harris, T. D.; Brus, L. E. *Nature* **1996**, *383*, 802−804.
(72) Norris, D. J.; Kuwata-Gonokami, M.; Moerner, W. E. *Appl. Phys. Lett.* **1997**, *71*, 297.
(73) Ormo, M.; Cubitt, A. B.; Kallio, K.; Gross, L. A.; Tsien, R. Y.; Remington, S. J. *Science* **1996**, *273*, 1392−5.
(74) Orrit, M.; Bernard, J. *Phys. Rev. Lett.* **1990**, *65*, 2716−19.

(75) Orrit, M.; Bernard, J.; Brown, R.; Lounis, B. Optical Spectroscopy of Single Molecules in Solids. In *Progress in Optics*; Wolf, E., Ed.; Elsevier: Amsterdam, 1996; Vol. 35, pp 61−144.

(76) Patterson, F. G.; Lee, H. W. H.; Wilson, W. L.; Fayer, M. D. *Chem. Phys.* **1984**, *84*, 51.

(77) Perkins, T. T.; Smith, D. E.; Chu, S. *Science* **1997**, *276*, 2016−2021.

(78) Peterman, E. J. G.; Brasselet, S.; Moerner, W. E. *J. Phys. Chem. A* **1999**, *103*, 10553−10560.

(79) *Amorphous Solids: Low-Temperature Properties*.; Phillips, W. A., Ed.; Springer: Berlin, 1981.

(80) Plakhotnik, T.; Donley, E. A.; Wild, U. P. *Annu. Rev. Phys. Chem.* **1996**, *48*, 181−212.

(81) Plakhotnik, T.; Moerner, W. E.; Irngartinger, T.; Wild, U. P. *Chimia* **1994**, *48*, 31.

(82) Rebane, K. K. *Impurity Spectra of Solids*; Plenum: New York, 1970.

(83) Reilly, P. D.; Skinner, J. L. *Phys. Rev. Lett.* **1993**, *71*, 4257−60.

(84) Reilly, P. D.; Skinner, J. L. *J. Chem. Phys.* **1995**, *102*, 1540.

(85) Sakmann, B.; Neher, E. *Single Channel Recording*; Plenum Press: New York, 1995.

(86) Schmidt, T.; Schutz, G. J.; Baumgartner, W.; Gruber, H. J.; Schindler, H. *Proc. Natl. Acad. Sci. U.S.A.* **1996**, *93*, 2926−29.

(87) Schwille, P.; Heikal, A. A.; Moerner, W. E.; Webb, W. W. *Proc. Natl. Acad. Sci. U.S.A.* **2000**, *97*, 151−156.

(88) Shera, E. B.; Seitzinger, N. K.; Davis, L. M.; Keller, R. A.; Soper, S. A. *Chem. Phys. Lett.* **1990**, *174*, 553.

(89) Skinner, J. L. Theoretical Models for Spectral Dynamics of Individual Molecules in Solids. In *Single Molecule Optical Detection, Imaging, and Spectroscopy*; Basché, T., Moerner, W. E., Orrit, M., Wild, U. P., Eds.; Verlag-Chemie: Munich, 1997.

(90) Skinner, J. L.; Moerner, W. E. *J. Phys. Chem.* **1996**, *100*, 13251−13262.

(91) Sosa, H.; Peterman, E. J.; Moerner, W. E.; Goldstein, L. S. B. *Nature Struct. Biol.* **2001**, *8*, 540−544.

(92) Stoneham, A. M. *Rev. Mod. Phys.* **1969**, *41*, 82.

(93) Svoboda, K.; Schmidt, C. F.; Schnapp, B. J.; Block, S. M. *Nature* **1993**, *365*, 721−727.

(94) Tamarat, P.; Lounis, B.; Bernard, J.; Orrit, M.; Kummer, S.; Kettner, R.; Mais, S.; Basché, T. *Phys. Rev. Lett.* **1995**, *75*, 1514.

(95) Tamarat, P.; Maali, A.; Lounis, B. L.; Orrit, M. *J. Phys. Chem. A* **2000**, *104*, 1−16.

(96) Tchénio, P.; Myers, A. B.; Moerner, W. E. *J. Phys. Chem.* **1993**, *97*, 2491.

(97) Tchénio, P.; Myers, A. B.; Moerner, W. E. *J. Lumin.* **1993**, *56*, 1.

(98) Tchénio, P.; Myers, A. B.; Moerner, W. E. *Chem. Phys. Lett.* **1993**, *213*, 325.

(99) Trautman, J. K.; Macklin, J. J. *Chem. Phys.* **1996**, *205*, 221−29.

(100) Trautman, J. K.; Macklin, J. J.; Brus, L. E.; Betzig, E. *Nature* **1994**, *369*, 40−42.

(101) Tsien, R. Y. *Annu. Rev. Biochem.* **1998**, *67*, 509−544.

(102) Visscher, K.; Schnitzer, M. J.; Block, S. M. *Nature* **1999**, *400*, 184−189.

(103) Vrjlic, M.; Nishimura, S.; Brasselet, S.; McConnell, H. M.; Moerner, W. E. (manuscript in preparation).

(104) Weiss, S. *Science* **1999**, *283*, 1676−1683.

(105) Wennmalm, S.; Edman, L.; Rigler, R. *Proc. Natl. Acad. Sci. U.S.A.* **1997**, *94*, 10641−10646.

(106) Wrachtrup, J.; Gruber, A.; Fleury, L.; von Borczyskowski, C. *Chem. Phys. Lett.* **1997**, *267*, 179.

(107) Wrachtrup, J.; von Borczyskowski, C.; Bernard, J.; Orrit, M.; Brown, R. *Nature* **1993**, *363*, 244.

(108) Xie, X. S. *Acc. Chem. Res.* **1996**, *29*, 9.

(109) Xie, X. S.; Trautman, J. K. *Annu. Rev. Phys. Chem.* **1998**, *49*, 441−480.

(110) Zumbusch, A.; Fleury, L.; Brown, R.; Bernard, J.; Orrit, M. *Phys. Rev. Lett.* **1993**, *70*, 3584.